A MULTI-DISCIPLINARY STUDY OF PORT ELIZA CAVE SEDIMENTS AND THEIR IMPLICATIONS FOR HUMAN COASTAL MIGRATION

by

Majid Hassan Mohammed Hassan Humaid Al-Suwaidi
B.Sc. (Honours), Earth Sciences
Brunel University, 2001

THESIS SUBMITTED IN PARTIAL FULFILLMENT OF
THE REQUIREMENTS FOR THE DEGREE OF

MASTER OF SCIENCE

In the School
of
Earth Sciences

SIMON FRASER UNIVERSITY

Spring 2005

APPROVAL

Name: **Majid Hassan Al-Suwaidi**

Degree: **Master of Science**

Title of Thesis: **A multi-disciplinary study of Port Eliza cave sediments and their implication for human coastal migration.**

Examining Committee:

Chair: **Dr. Peter Mustard**
Associate Professor Department of Earth Science.

Dr. Brent Ward
Senior Supervisor
Associate Professor Department of Earth Science

Dr. John Clague
Supervisor
Professor Department of Earth Science

Dr. James MacEachern
Supervisor
Associate Professor Department of Earth Science

Dr. Lionel Jackson
External Examiner
Researcher Geological Survey of Canada

Date Defended/Approved: Jan 31 2005

SIMON FRASER UNIVERSITY

PARTIAL COPYRIGHT LICENCE

ABSTRACT

A multi-disciplinary study at Port Eliza cave on Vancouver Island has refined the timing and character of late Wisconsinan environments and has significant implications for the Human Coastal Migration Hypothesis. Loss-on-ignition, paleomagnetic and sedimentological data show that there was continuous sedimentation through the last glacial maximum, implying a warm-based Cordilleran Ice Sheet. Radiocarbon dating supported by paleomagnetic data and U/Th ages constrain the time of maximum glaciation to between *ca.* 16 and 12.5 ka BP. Terrestrial floral and faunal data indicate a pre-Last Glacial Maximum, cold, dry, steppe environment with rare trees but a diverse fauna. Marine fossils represent a rich, dominantly nearshore fauna and suggest the sea was close to the cave. These data indicate that ice-free conditions lasted until at least 16 ka BP, and suggest that prior to the late Wisconsinan glacial maximum, humans could have survived on a mixed marine-terrestrial diet in the Port Eliza area.

DEDICATION

To my parents Joanne and Hassan

ACKNOWLEDGEMENTS

First and foremost I would like to thank Dr. Brent Ward without whom this thesis would not have been possible. He supported me tirelessly and I feel honoured to have had him as a supervisor and to count him as a friend.

I would like to extend a special thanks to Dr. Mike Wilson who helped in writing and editing chapter three and who's support was invaluable. Also to Dr. Randy Enkin who helped with the writing and editing of chapter four and who guided me through the world of palaeomagnetism. A special thanks also to Dr. Bassam Ghaleb and Dr. Dan Marshall from whom I learned so much.

Fossil mammal and bird bones were identified by Dr. Mike Wilson and Dr. D. Nagorsen, and B. Wiggen identified the fish bones. Dr. Paul Matheus, confirmed the Townsend's vole identification. Uranium-thorium dating was carried out at the GEOTOP-UQAM-McGill in collaboration with Dr. B. Ghaleb, and paleomagnetic analysis was carried out at the Pacific Geoscience Centre under the direction of Dr. R. Enkin and Judith Baker. SEM and X-Ray diffraction samples were processed and analysed at Simon Fraser University under the direction of Dr. D. Marshal. C. Kowalchuk, S. Villeneuve, and D. Parks provided assistance in the field and laboratory. I also thank Mathew Plotnikoff, for help with grain size analysis, Dr. Duane Froese, arranged the processing of grain-size samples by sedigraph at the University of Alberta, and Dr. Brian Menounos, prepared some of the thin sections at the University of British Columbia. I would also like to thank the Ehattesaht Nation, specifically Sharon Elshaw and Lyle Billy, for allowing this research to be conducted on their traditional territories. Western Forest Products and Taylor Contracting provided logistical support.

Thanks also to my fellow graduate students for their support and camaraderie. In particular; Dan Utting, Crystal Huscroft, Chris Kowalchuk, Tom Gleeson and Julianne Madsen all of whom helped through discussion and in editing of this thesis. Last but not least I would like to thank Kenna Wilkie for her amazing patience and support.

TABLE OF CONTENTS

LIST OF FIGURES

LIST OF TABLES

CHAPTER ONE

INTRODUCTION

During the Pleistocene, the Cordilleran Ice Sheet repeatedly covered all of British Columbia, and parts of Yukon and northwestern USA. Each advance largely removed the evidence of previous glacial and non-glacial periods, rendering a reconstruction of the history of pre-Last Glacial Maximum (LGM) environments challenging.

The late Wisconsinan glaciation of British Columbia is of particular interest, as it bears on discussions of human migration to North America. The "Clovis-first" hypothesis (Johnston, 1933) has been the accepted model for human migration since the 1930's. According to this hypothesis, early Clovis people travelled along an ice-free corridor between the Cordilleran and Laurentide Ice Sheets and rapidly colonised all of North and South America (Mandryk *et al.*, 2001; Jackson and Wilson, 2004). The Monte Verde site of southern Chile (12.5 ka BP; unless otherwise stated all dates are in radiocarbon years before present) pre-dates the North American Clovis record by 1,300 years (Meltzer *et al.*, 1997). This necessarily pushes human migration further back to allow migrants time to reach southern Chile. Studies along the northern (Duk-Rudkin and Hughes, 1991, 1992) and southern (Jackson *et al.*, 2001) margins of the Laurentide and Cordilleran ice sheets indicate coalesence during the late Wisconisnan. The recent compilation by Dyke (2004) indicates the corridor would have opened after 12.5 or 12 ka BP. This allows the possibility of Clovis people migrating through the area, although the environmental condition at this time may not have been viable for humans (Mandryk *et al.*, 2001). Nevertheless, the antiquity of the Monte Verde site still indicates that people could not have travelled via the ice free Corridor as it was just opening at this time. The conflict between

the Monte Verde site and the "Clovis-first" hypothesis has prompted a re-examination of an alternative; the coastal migration hypothesis (Fladmark, 1983).

The coastal migration route was once thought to be blocked by an extensive Cordilleran Ice Sheet, however, recent work implies that it was viable (Blaise *et al.*, 1990; Mann and Peteet, 1994; Heaton *et al.*, 1996; Josenhans *et al.*, 1997; Barrie and Conway, 1999; Fedje and Josenhans, 2000; Hetherington *et al.*, 2003; Ward *et al.*, 2003; Hetherington *et al.*, 2004). More data, however, are required to confirm times of ice advance and retreat and environmental conditions during the period of human colonisation of the Americas (Mandryk *et al.*, 2001). This thesis helps to elucidate the late Wisconsinan environments of the west coast of Vancouver Island through an examination of sediments at Port Eliza cave, Vancouver Island (Figure 1.1). This chapter outlines the objectives of the thesis and pertinent previous research. The chapter closes with an outline of the thesis.

Objectives

Sediments preserved in raised sea caves in Norway have provided a long record of glacial events and associated palaeoenvironments (Larsen *et al.*, 1987; Valen *et al.*, 1996). The west coast of Vancouver Island is an ideal area for this type of research. Long stretches of coastline are exposed to frequent storms that are forming wave-cut caves, and many old caves have been elevated above the present shore. This study uses one elevated wave-cut cave to develop an improved chronology of the last glacial maximum. The objectives of the study were to:

1. document sediments preserved within Port Eliza cave, with the aim of establishing environments of deposition.

2. To apply multi-disciplinary methods to reconstruct environments of deposition and date the sediments.

3. To determine the timing and character of late Wisconsinan glaciation and the late Wisconsinan nonglacial interval and

4. identify and interpret the fossil fauna and flora of pre-LGM sediments; and

5. comment on the viability of a coastal migration route for early human migration into North America.

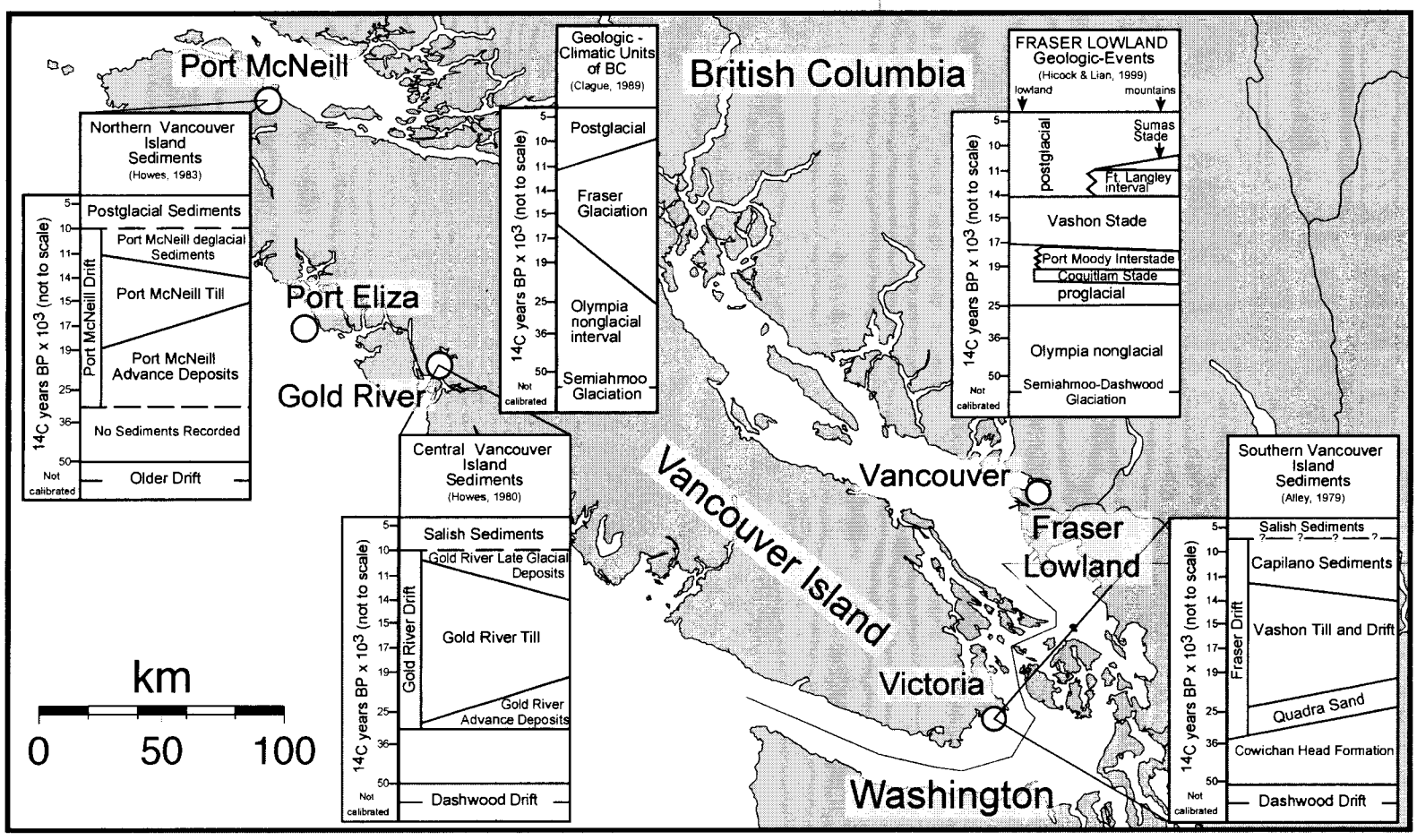

Figure 1.1. Location of Port Eliza, and the late Pleistocene stratigraphy of Vancouver Island and the Fraser Lowland.

Background

Larsen and Mangerud (1989) suggest that uplifted wave-cut caves, which lie above the post-glacial marine limit, can provide a long history of glacial and non-glacial events. Sequences of alternating fine-grained and blocky (cave-roof-fall) sediments in caves can be used as on-off signals of glaciation. During glacial periods caves are blocked by ice and filled with water, resulting in deposition of fine-grained sediments. During nonglacial periods, caves are open and undergo weathering, giving rise to blocky deposits and, under some conditions, speleothems. Animals are likely to inhabit the caves during non-glacial periods, leaving bones within the blocky facies. Valen *et al.* (1996) in the Hamnsundhellern cave, western Norway, found more than 15,000 bones, providing paleoenvironmental data and chronologic control.

Several methods can be used to develop chronologies and obtain paleoenvironmental information in wave-cut caves. The fine-grained facies is an excellent recorder of the Earth's magnetic field. Comparison of secular variation recorded in these sediments with that from well-dated reference sites can provide chronological control (Larsen *et al.*, 1987) and correlation. Valen *et al.* (1995) for example correlated sediments in the Olahola and Skjonghelleren caves in western Norway by using magnetostratigraphy. Bones in the blocky facies can be used for paleoenvironmental study and radiocarbon dating. Speleothems can be dated by U-series methods, which allow the record to be extended beyond the range of radiocarbon dating. The potential for dating both glacial and non-glacial deposits makes caves excellent sites for refining the glacial record.

Glacial history of the Fraser Lowland and Vancouver Island

Late Quaternary geologic-climatic units for southwestern B.C. include the late Wisconsinan Fraser Glaciation, the middle Wisconsinan Olympia nonglacial interval, and the

penultimate Semiahmoo-Dashwood glaciation (Figure 1.1). In the Fraser Lowland, the Fraser Glaciation includes three stades, from oldest to youngest, the Coquitlam, Vashon and Sumas stades (Armstrong & Clague, 1977; Armstrong, 1981; Clague *et al.,* 1980, 1989; Hicock & Armstrong, 1981; Lian & Hickin, 1993; Hicock and Lian, 1995 and Clague *et al.,* 1997). In contrast, only one stade has been recognized on Vancouver Island (Howes, 1981, 1983; Alley, 1979).

The Fraser Lowland

The earliest stade of the Fraser Glaciation is the Coquitlam (Hicock and Armstrong, 1981). Fraser Lowland ice blocked the Coquitlam Valley and other north shore valleys from 21.5 ka BP until *ca.* 18.7 ka BP. The Coquitlam Stade was followed by the Port Moody Interstade, dated between 18.7ka and 17.6 ka BP (Hicock and Lian, 1995; Figure 1.1). Lian *et al.* (2001) argue that this interval was one of global warmth, as it is recorded in Greenland ice cores. Palynological and plant macrofossil data indicate a subalpine forest parkland environment with extended cold winters and short dry summers, near present sea level near Vancouver during the Port Moody Interstade (Hicock and Lian, 1995). Lian *et al.* (2001), however, suggest a temperate, moist climate at this time. They use the pollen of *Typha latipholia*, to infer mean July temperatures exceeding 13°C. The Vashon Stade followed the end of the Port Moody Interstade and represents the peak of the Fraser Glaciation, when, about 14.5 ka BP, the Cordilleran Ice Sheet reached its maximum extent.

Vancouver Island

Valley glaciers were advancing on Vancouver Island before 25 ka BP (Howes, 1981). Vancouver Island also shows evidence of a single late Wisconsinan advance, which has been correlated with the Vashon Stade of the Fraser Lowland (Figure 1.1). Near the peak of the Fraser

Glaciation, *ca.* 15 ka BP (Clague *et al.,* 1980; Clague and James, 2002), the Cordilleran Ice Sheet coalesced with, and eventually over-topped ice derived from Vancouver Island (Howes, 1983). The Tofino area, on the west coast of Vancouver Island, was not overridden by glaciers until some time after 16.7 ka BP (Blaise *et al.*, 1990).

Location and regional geology

Port Eliza cave is located on the northwestern coast of Vancouver Island, northwest of Nootka Island, at the entrance to Esperanza Inlet (Figure 1.1). The area consists of rocky headlands separated by sand and gravel beaches. Elevations in the area of the cave range from 0 to 2100 m in the headwaters of the local watersheds. Steep areas are dominantly rock, whereas areas of lower relief are draped with glacial and post-glacial sediments. The cave is 85 m above present-day sea level about 50 m above the post-glacial marine limit of ca. 35m (Clague and James, 2002).

Vancouver Island is underlain by both granitoid rocks of the West Coast Complex and Mesozoic (upper Triassic and Lower Jurrassic) arc-type volcanics and sediments, all intruded by numerous Eocene batholiths (Muller *et al.*, 1974). Port Eliza cave formed in Lower Jurrassic, Bonanza Group rocks of the Eliza Dome (Muller, 1977). These consist of basaltic to rhyodacitic lavas, tuffs, breccias, and include some greywacke and siltstone deposits. Locally (in the vicinity of Port Eliza), there are Middle and Upper Jurassic siltstones, shale, greywacke, and conglomerate of the Kapoose Formation, as well as Lower Jurassic Island intrusions of granodiorite, quartz diorite and granite.

Thesis format

This thesis contains two journal-style papers. Each paper focuses on a different aspect of the research at Port Eliza cave. To prevent repetition, the methods applied in this research have been extracted from the two papers and are presented in Chapter Two.

The first paper (Chapter Three) focuses on the paleoenvironmental implications of the sediments and fossils at Port Eliza cave. Recently there has been a debate concerning human migration into North America and the viability of a coastal route (Mandryk *et al.*, 2001). The location of Port Eliza cave along the proposed migration route allows the research at the cave to contribute to this debate. Data from the cave constrains the time of glaciation and provides information on the pre-LGM environment. This paper has been submitted to the Journal of Geoarchaeology and is currently under review.

The second paper (Chapter Four) focuses on the origin of the fine-grained sediments in Port Eliza cave and their paleomagnetic signature. The record of secular variation is correlated to records to the south, providing an approximate age for the fine-grained sediments. This paper will be submitted to CJES.

Chapter Five summarises the main points of the thesis and discusses them in relation to the late Wisconsinan record of Vancouver Island and the Fraser Lowland.

CHAPTER TWO

METHODS

Fieldwork

Fieldwork was carried out at Port Eliza cave from 2000 to 2002. Results from the 2000 and 2001 field seasons were published by Ward *et al.* (2003). These results are synthesised with new data collected during the summer of 2002, during which a more comprehensive study of the cave sediments was made.

Water had to be pumped from the excavation made in 2001 before work could commence in 2002. The excavation was then widened to approximately 1 m and deepened to approximately 3 m. The sediments were described, measured and photographed in detail to produce a lithologic log (Appendix A). Bulk samples of the basal diamicton were collected in 10 cm increments using a hammer and chisel, to a depth of 80 cm. Cohesive block samples were collected from the fine-grained unit for detailed laboratory analysis, including texture, mineralogy, paleomagnetism, pollen, and organic content. Moist sediment colours were described in the field using a Munsell soil colour chart.

Granulometric analysis

Granulometric analyses of bulk, coarse-grained sediment samples were carried out using the hydrometer method (Gee and Bauder, 1986). Samples of fine-grained sediment were processed using a Micromeritics sedigraph 5100 at the University of Alberta. The Wentworth scale was used to classify sediment: sand >62.5 μm; silt <62.5 μm to >3.9 μm; and clay <3.9 μm.

Sand size and coarser sediment (>62.5 μm) were dry sieved using standard methods (Appendix B).

X-ray diffraction analysis

Selected clay subsamples from the fine-grained unit were analysed using an X-ray diffractometer to determine mineralogy. The subsamples were chosen based on dominant colours of laminations. Samples were dried overnight at 150 °C, powdered using a mortar and pestle, and compacted onto a glass slide holder. A Philips model PW1730 defractometer with a Ni-filtered Cu Kα (λ=1.542) radiation tube was used at operating conditions of 40 KeV and 25 mA. Each sample was analyzed across a range of 2θ angles from 5° to 65°. Count times of 2 and 10 seconds were used, at step sizes of 0.05 and 0.02 (Appendix C). Mineral peaks were identified with the help of Dr. Dan Marshall, using the Joint Committee on Powder Diffraction Standards Database (JCPDS, 1993).

Scanning electron microscopy analysis

A Bausch and Lomb NANOLAB LE 2100 scanning electron microscope (SEM) equipped with a Kevex energy dispersive spectral (EDS) analyzer, Bauch and Lomb secondary electron (SE) detector, backscattered electron (BE) detector and cathode luminescence (CL) detector was used to analyze quartz grain morphologies. Subsamples of loose matrix were collected from selected intervals within diamicton units, mixed in de-ionized water, and left for 60 seconds to separate the sand fraction from the fines. A first batch of samples was agitated in a hydrosonic bath for 1 minute intervals to remove adhering clay particles and then dried (Appendix D). A second batch of samples were boiled in concentrated HCL, further washed with calgon, and then dried (Appendix D). The dried grains were mounted on standard half-inch SEM stubs with double-sided carbon tape, and coated with approximately 200 angstroms of carbon.

The SEM samples were observed using accelerating voltages of 10 or 15 KeV. Beam currents were generally less than 0.1 nanoamperes for imaging and approximately 1.0 nanoamperes for EDS analyses. EDS analyses and semiquantitative identification of quartz grains were performed using Desktop Spectrum Analyzer (DTSA) software developed by the U.S. National Institute of Science and Technology (NIST) with an Aptec Flat Pack to condition the EDS detector signal. SE, BE and CL images were collected using a software package developed by the U.S. National Institute of Health. These analysis were carried out under the supervision of Dr. Dan Marshall.

Uranium/Thorium dating

Uranium-series dating was carried out at GEOTOP-UQAM-McGill, Montreal, under the direction of Dr. Bassam Ghaleb. Analyses were carried out both by thermal ionisation mass spectrometry (TIMS) and alpha spectrometry. Individual dripstone fragments were cleaned by mechanical abrasion and, after the addition of a spike (^{233}U-^{236}U-^{229}Th), were dissolved in 7N HNO_3. Further processing was carried out using protocols defined by Edwards *et al.* (1987). The uranium and thorium were separated from the bulk of the material with $Fe(OH)_3$ and from more similar elements of the actinides group by absorption in a Dowex AG1-X8 ion exchange using standard techniques (Ivanovich and Harmon, 1992). Uranium and thorium were loaded on an outgassed, zone-refined, graphite-coated rhenium filament. The concentration and isotopic composition of U and Th were measured by TIMS, using a VG Sector mass spectrometer, equipped with a 10 cm electrostatic analyzer and a pulse-counting Daly detector (Appendix E). Mass fractionation was corrected for by normalizing to the known $^{236}U/^{233}U$ ratio (1.14) in the double spike. U concentrations were low, and the presence of minor amounts of contamination from detrital material from the enclosing diamicton required correction.

The results of ^{232}Th, $^{230}Th/^{232}Th$, $^{238}U/^{232}Th$, and $^{234}U/^{232}Th$ from the diamicton samples are considered to represent the detrital end member and were used to correct the results from the

dripstone samples. Diamicton samples were processed by alpha spectrometry by Dr Bassam Ghaleb. Each sample was powdered and approximately 1g used for determination of U-Th isotopic composition and concentration. A spike of ^{232}U-^{228}Th at secular equilibrium was added and evaporated for yield determination. After a complete digestion of the sample with aqua regia and a mixture of concentrated HF-HNO_3 it was evaporated until dry. The sample was then re-dissolved with 6M HCl, and uranium and thorium were separated from the bulk of the material with $Fe(OH)_3$, and from more similar elements of the actinides group by absorption on a Dowex AG1-X8 ion exchange using standard techniques(Ivanovich and Harmon, 1992). The final fraction of U and Th was electroplated onto silver discs and counted in a EGG-Ortec-476 alpha spectrometer. The overall analytical reproducibility is better than ± 0.5%, and was estimated from replicate measurement of a coral from Timor Island of the last interglacial age (O-isotope sub stage 5e) and of a uraninite standard.

Paleomagnetic analysis

Plastic cylinders and a u-channel were tapped gently into a clean vertical face of fine-grained sediment and their orientations measured using a Brunton compass. As the unit contained faults, care was taken to sample the largest fault-bound blocks to ensure internal consistency. Duplicate samples were taken across faults to check for differential movement between blocks. Paleomagnetic remanence was measured at the Geological Survey of Canada - Pacific on an AGICO JR5-A spinner magnetometer under the direction of Dr. Randy Enkin and Judith Baker. Analysis of the u-channel was carried out by Dr. K. Verosub at the University of California, Davis. Stepwise alternating field demagnetization was carried out using a Schonstedt GSD-5 with tumbler in peak fields up to 100 mT, with 3 to 8 steps. The remanence was strong (0.2 to 5 A/m) and stable (median destructive field between 60 and 100 mT), indicating that fine-grained magnetite is the magnetic carrier (Appendix F).

Radiocarbon dating

Single bone fragments of known species were selected for AMS dating. Collagen of high molecular weight was extracted and CO_2 produced by it's combustion was collected at SFU by Cheryl Takahashi under the direction of Dr. Erle Nelson. Extraction yields and C/N ratios indicate that the collagen was moderately well preserved. The CO_2 was sent to Lawrence Livermore for AMS analysis. ^{13}C values, and C and N concentrations were measured at UBC. All samples display typical ^{13}C values for terrestrial animals with the exception of the sparrow bone, which could reflect a small amount of marine carbon, possibly as a result of its diet. Despite this, any correction for this effect would lie within the range of uncertainties. All measured radiocarbon ages (given at 1 sigma) were converted to calendrical ages (cal BP at 1 sigma) using the program CALIBv4.0 (Stuiver and Reimer, 1993; Stuiver *et al.,* 1998). All ages presented in this thesis are in ^{14}C radiocarbon years BP unless otherwise noted.

Loss-on-ignition analysis

Samples from fine-grained sediments were measured for organic and inorganic carbon. One ml subsamples, collected at 2 cm intervals, were dried overnight in crucibles at 150 °C. They were then fired at 550 °C and 950 °C each, for 2.5 hrs in a muffle furnace according to a procedure defined by Smith (2003) for clay-rich glaciolacustrine sediments (Appendix G).

Thin-section analysis

Fine-grained sediments were mounted in resin for thin-section analysis at the University of British Columbia. Slabs 1 cm by 12 cm were cut, then frozen in liquid nitrogen, before being placed in a desiccator. The samples were then covered with low-viscosity spurr resin and left to cure under vacuum. The hardened samples were cut to thin sections for examination (Menounos, 2002). A second set of samples were processed using acetone replacement, based on the method

of Fitzpatrick (1984, 1993) and Menounos (2002). Samples were soaked in acetone for fourteen days and replaced each day for the first seven days, and then on alternate days for the remaining seven days. Following this, the acetone was drained and the samples were covered in rigid urethane casting resin before being placed under a low vacuum for two hours. The samples were then cured for 24 hours at low temperatures in a fan-assisted oven (Appendix H).

Pollen analysis

Sediments were prepared by a standard protocol. Silicates were removed from samples by treatment with warm concentrated HF. Following conventional acetoylsis (Faegri and Iversen, 1989), the residue was screened through a 15 μm mesh. Pollen and spore concentrations were not determined because of the heterogeneous character of the sediment; the variation in grain size between samples would impart a difference in concentration not reflective of the true pollen concentration. Identifications were made by comparison to standard reference works, an unpublished key to pollen and spores of British Columbia, and the pollen and spore reference collection at the Royal British Columbia Museum. Analysis was carried out by Dr. Richard Hebda, of The Royal B.C. Museum (Appendix I).

Bone analysis and identification

Samples of basal diamicton were disaggregated in tap water and sieved using a series of nested screens. Bones and bone fragments were picked out of the different size fractions, cleaned in ultra-distilled water in a hydrosonic bath, and then air dried. Dr. Michael Wilson, Douglas College, carried out the bulk of the identifications. Some mammals were identified by Dave Nagorsen, Mammalia Biological Consulting, Victoria, and the fish were identified by Becky Wigen, Department of Anthropology, University of Victoria. Identification was aided by

comparison to reference collections at Simon Fraser University, the University of Victoria, and The Royal B.C. Museum.

CHAPTER THREE

LATE WISCONSINAN PORT ELIZA CAVE DEPOSITS AND THEIR IMPLICATIONS FOR HUMAN COASTAL MIGRATION, VANCOUVER ISLAND, CANADA*.

Introduction

There has recently been a debate concerning the viability of a coastal migration route as an alternative to the inland "Ice-Free Corridor" hypothesis (e.g. Mandryk *et al.*, 2001). Acceptance of early human settlement at Monte Verde, Chile, dated to *ca.* 12,500 BP (Dillehay, 1989, 1997; Adovasio and Pedler, 1997; Meltzer, 1997), necessarily pushes the onset of human arrival to North America further back in time, to allow time for travel from Beringia to South America (Mandryk *et al.*, 2001).

The "Ice-free Corridor" hypothesis was developed in the 1930s, following the discovery of late Pleistocene Clovis culture sites east of the Cordillera. This postulated route necessitated a gap between the Laurentide and Cordilleran ice sheets that extended from the Yukon Valley into the Mackenzie watershed and down the eastern edge of the Rockies (Johnston, 1933; Mandryk *et al.*, 2001; Jackson and Wilson, 2004). The alternative "coastal migration route" hypothesis envisions early paleoindian groups traversing an emergent continental shelf when sea level was lower than present, likely assisted by watercraft. This proposed route extends from the Bering Strait, along the southern coast of Alaska and down the British Columbia coast (Fladmark, 1979;

* A version of this chapter has been accepted in the journal of Geoarcheology and was co-authored with Ward B.C, Hebda R.J., Nagorsen D.W., Marshall D., Ghaleb B., Wigen R.J., and Enkin R.J.

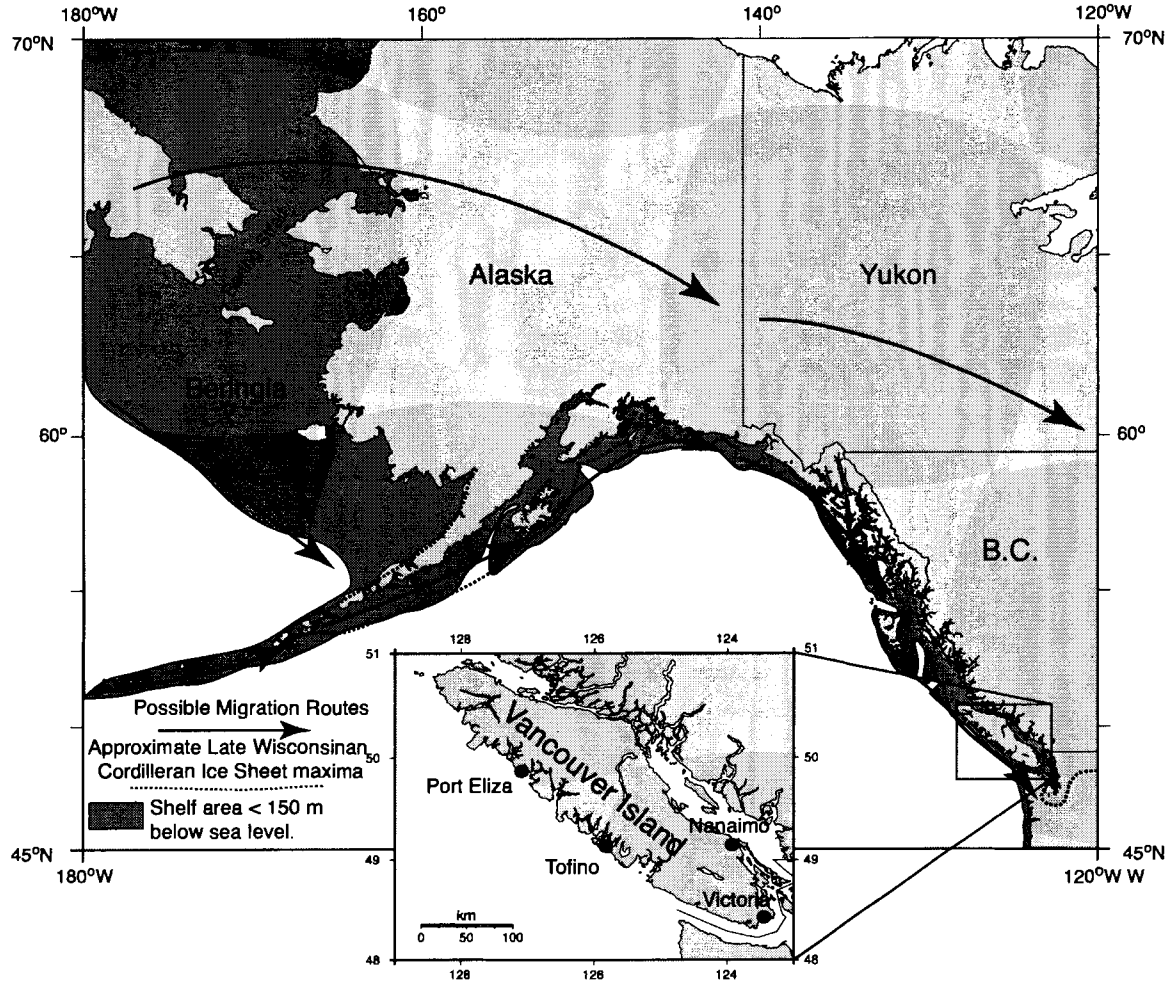

Figure 3.1. Location of Port Eliza cave along the hypothesised "coastal migration route". Cordilleran Ice Sheet limit after Blaise *et al.* 1990; Mann and Kaufman, 2002

Dixon, 1999) (Figure 3.1). Evaluation of the viability of either route has until recently suffered from a paucity of direct evidence. To help address this knowledge gap, this paper presents results of field studies carried out in Port Eliza cave, Vancouver Island, which lies along the proposed coastal route. The research shows that glacier ice did not cover the outer coast of the island until after 16.3 ka BP, and that conditions immediately before this would have permitted human migration.

Background and setting

The Cordilleran Ice Sheet periodically dominated the Quaternary landscape of British Columbia, Yukon, western Alberta, and portions of the northwestern United States. It comprised valley and piedmont glaciers, as well as mountain ice sheets (Clague, 1989). The last ice sheet, present during the late Wisconsinan Fraser Glaciation, has been extensively studied throughout B.C. Two advance stades, the Coquitlam and Vashon, separated by the Port Moody Interstade, have been recognised in the Fraser Lowland (Figure 3.2). The Sumas Stade is a late glacial re-advance (Hicock and Lian, 1995).

The impetus for investigation of cave sites in this area was drawn from seminal research carried out in Norway, that established raised sea caves as invaluable sources of direct data for paleoenvironmental studies of past glaciations (Larsen *et al.*, 1987; Valen *et al.,* 1996). Raised sea caves form by wave action along exposed coastlines during periods of higher relative sea level. If the caves occupy positions above the post-glacial marine limit, they can preserve a distinctive stratigraphy that records alternating glacial and nonglacial conditions. During glaciations the cave entrance is blocked by ice, and the cave fills with glacial meltwater, forming a subglacial lake, in which stratified silt and clay sediments are deposited (Figure 3.3). In some cases, ice may extend into the cave, depositing till. During nonglacial periods, gravity and freeze-thaw action leads to rock fall accumulations on the cave floor, possibly accompanied with

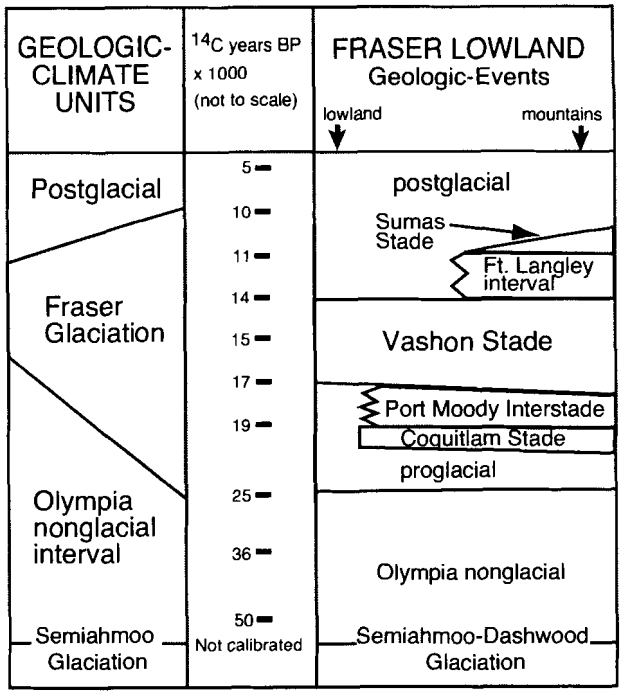

Figure 3.2. Late Quaternary geologic climate units and events of southwestern British Columbia (modified from Hicock and Lian, 1995)

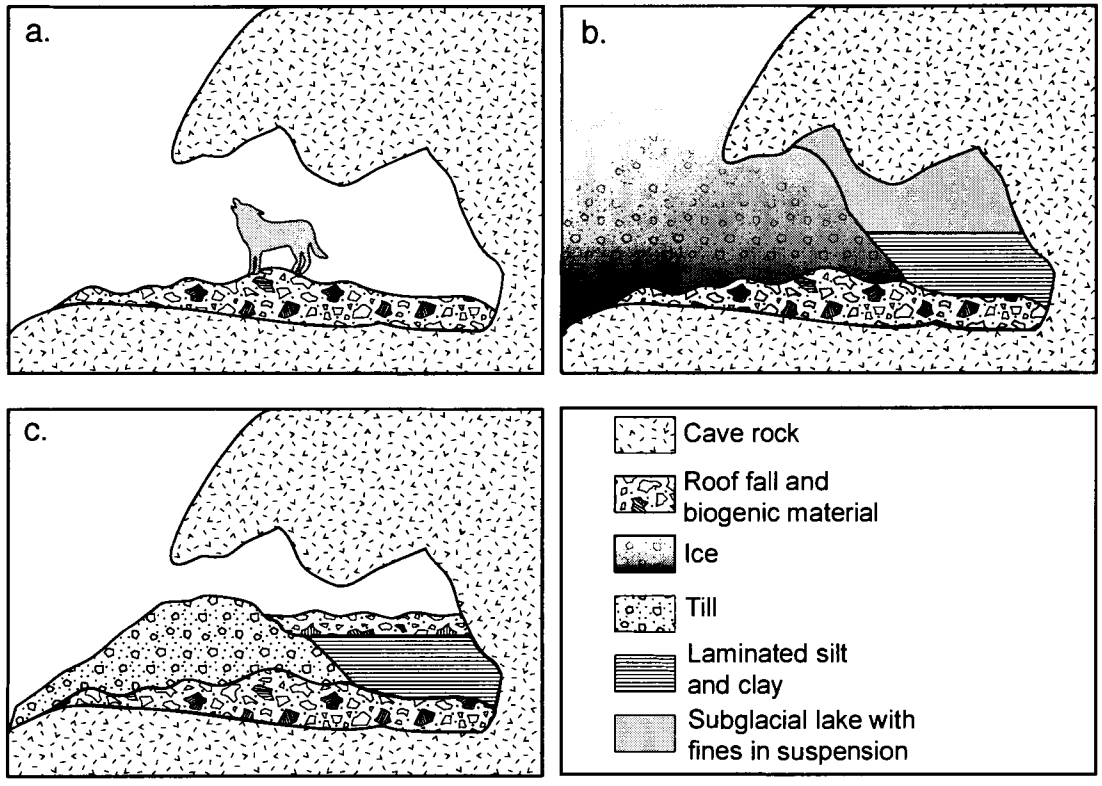

Figure 3.3. Schematic model of glacial-non-glacial cave sedimentation, based on Larsen *et.al.* (1987); a. under initial, open cave conditions the cave floor acculmulates material from roof fall and animal occupation; b. during subsequent glaciation the cave entrance is blocked by ice and fine-grained sediment is deposited within the cave as well as till at the entrance; c. after deglaciation the cave returns to open conditions and the accumulation of roof fall and biogenic material.

speleothem formation (precipitated from groundwater). Bone material is commonly found in association with these units, and coupled with the speleothem deposits, can provide both chronological control and paleoenvironmental data.

Port Eliza cave

Port Eliza cave is situated on the northern end of the west coast of Vancouver Island (Figure 3.1) and was formed by wave action exploiting a fault in Jurassic-aged volcanic rocks of the Bonanza Group (Muller, 1977). The cave is approximately 85 m above present-day sea level, lying well above the local post-glacial marine limit of 35 m (estimated based on Clague and James, 2002). The cave is 60 m long, and ranges in height from less than 1 m to 15 m (Figure 3.4). The floor is covered with large angular blocks near the entrance, and has standing water above fine-grained material toward the back, with areas of dripstone. The cave walls support speleothems including soda straws and stalactites.

Lithostratigraphy

Lithostratigraphic units are presented in terms of sediments of the "interior cave complex" (Units *I*- 1 through 4) and sediments of the "cave entrance complex" (Units *E*- 1 and 2) (Figure 3.4).

Sediments of the interior cave complex

Unit *I*-1

Unit *I*-1 is a well-indurated, largely unsorted, matrix-supported diamicton (Figure 3.5a). It was excavated to a depth of approximately 80 cm, but the lower contact was not observed. The upper surface is irregular; it is concave over the 1.5 m described, dropping 15 cm in the center,

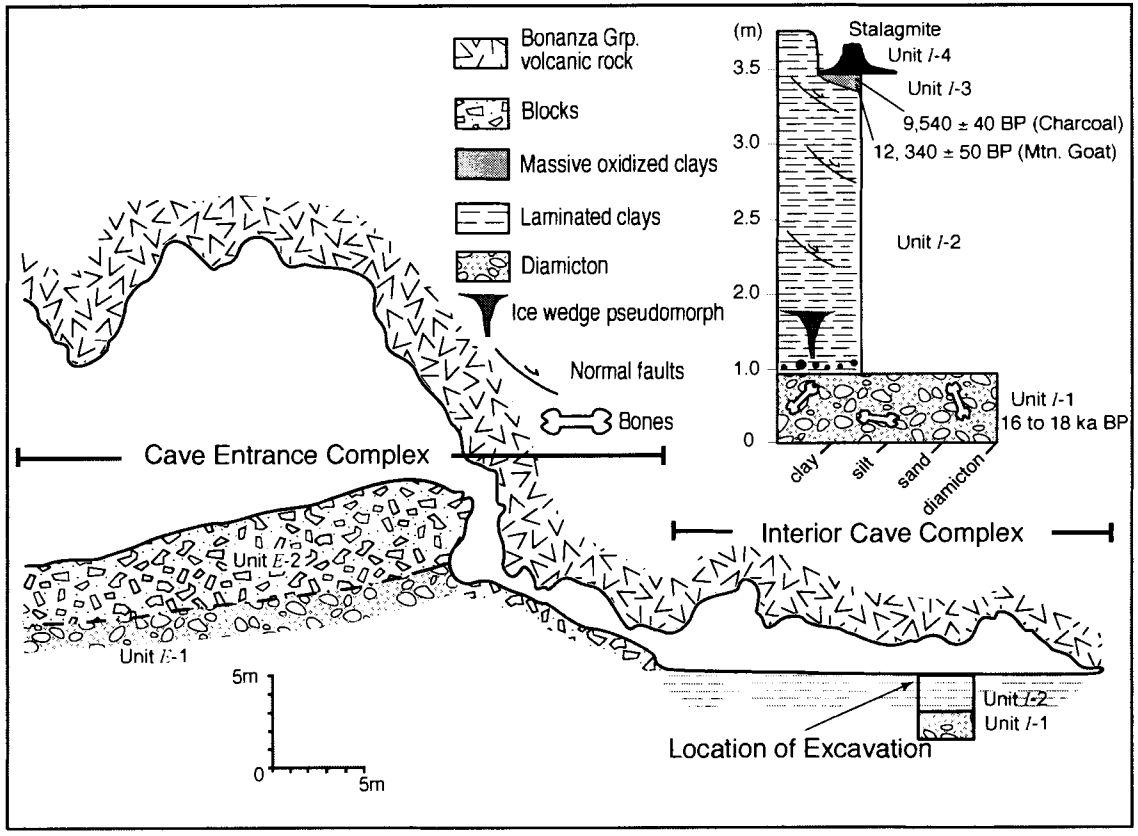

Figure 3.4. Cross-section and stratigraphy of Port Eliza cave.

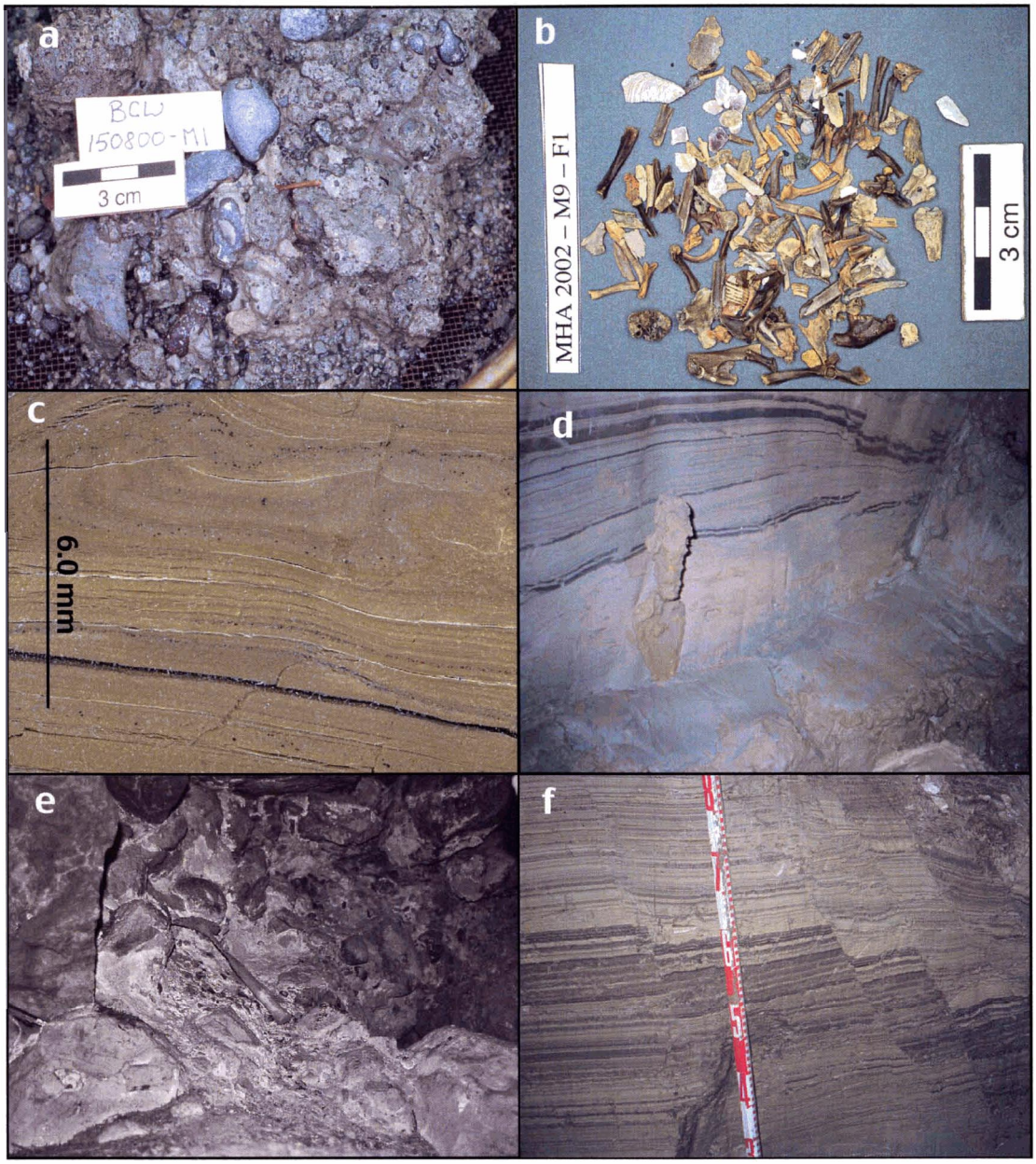

Figure 3.5. a. diamicton from Unit *I*-1; b. selection of bones from Unit *I*-1; c. thin-section of Unit *I*-2 laminations with some convolutions; d. distinctive dark beds in massive clay of Unit *I*-2 (trowel is 26 cm long and point is on lower contact) e. diamicton of Unit *E*-1; rock hammer is 35 cm long; f. faulting in laminated silt and clay of Unit *I*-2.

with relief of 4-5 cm over distances of 10-15 cm. The unit contains approximately 30% clasts of different lithologies, including local cave rocks and exotic clasts of porphyritic granite, metamorphic rocks, and various siltstones and sandstones. Local clasts are angular to subangular, whereas exotic clasts are subangular to rounded and display the full range of sphericity. Clasts range in length from <1 cm to >19 cm (clasts >19 were not collected). The average size of clasts separated from bulk samples of diamicton is 1.9 cm. The modal size is 0.4 cm. Dripstone fragments up to 6 cm were also found within this unit.

The matrix of Unit *I*-1 is dominantly sand-sized material, with samples averaging 60% sand and 14% silt (Figure 3.6). There is little observed structural or textural variability in the unit, but two indistinct zones are noted. In the upper zone (approximately 10 to 15 cm thick) sediments are unsorted and fissile, with faint vestiges of bedding. This zone is light grey (all colours are from Munsell Soil Colour Chart), and has a finer grained matrix (only 20% sand and silt) with fewer granules than the sediments below. The lower zone of the diamicton is also unsorted, but is massive and dark brown in colour. Surface morphologies of quartz grains isolated from the matrix vary little throughout the excavated material. Grains are angular and conchoidally fractured, with some showing evidence of crushing (Figure 3.7).

Unit *I*-1 contains numerous small bones, many of which are intact and with little wear. They occur randomly throughout the thickness sampled, with no vertical variation in concentration noted (Figure 3.6). They range in colour from white to dark brown, and their surfaces are fresh to weathered. Brown-stained specimens are darker and more common at depth. Shell fragments are also present in Unit *I*-1 and are most common in the lowest 10 cm sampled.

Radiocarbon ages from this unit range from 18.0-16.3 ka BP (Table 3.1). U-series ages on two dripstone fragments are 16 and 14 ka BP (Table 3.2).

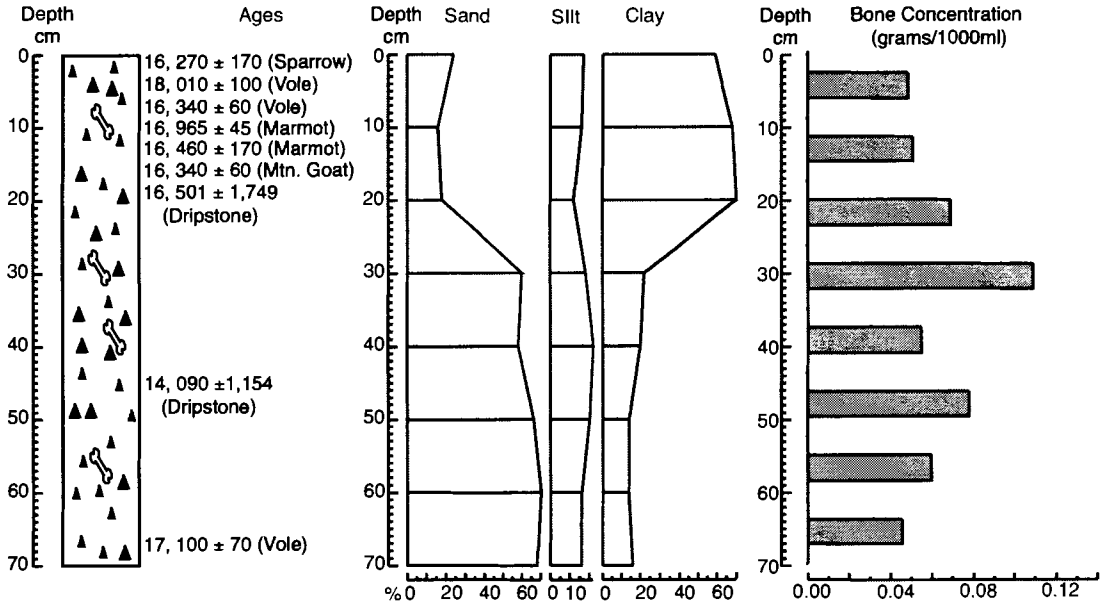

Figure 3.6. Radiocarbon ages, grain-size, and bone concentrations in Unit *I*-1.

Table 3.1 Radiocarbon ages from Port Eliza cave

CAMS# [ϕ]	Unit	Material[φ]	Weight (mg)	$\delta^{13}C$ (‰ vPDB)	^{14}C age (BP)	Calendar age (calBP)
74626	*I*-3	Charcoal	15.3	-25.5	9,540±40	11,065 –10,940
97342	*I*-3	Mountain Goat	79.1	-19.8	12,340±50	15,035-14,615 and 14,405-14,120
88275	*I*-1	Sparrow	45.0	-18.6	16,270±170	19,720-19,010
74625	*I*-1	Vole	43.3	-20.9	16,340±60	19,790-19,180
102798	*I*-1	Mountain Goat	51.3	-19.5	16,340±60	19,790-19,180
88274	*I*-1	Marmot	46.2	-20.5	16,460±170	19,970-19,250
97341*			77.5		16,965±45	20,520-19,885
102797	*I*-1	Vole	67.6	-19.7	17,100±70	20,685-20,030
74624	*I*-1	Vole	41.1	-20.2	18,010±100	21,750-21,060

* Duplicate analysis of same bone fragment.

[ϕ] Lawrence Livermore laboratory

[φ] All bone dates were on collagen

Table 3.2 Uranium series ages from dripstone in Unit *I*-1

Sample	Subsample and location	Method	[^{238}U] ppb	[^{232}Th] ppt	(^{234}U/^{238}U) activity ratio	(^{230}Th/^{234}U) activity ratio	(^{230}Th/^{232}Th) activity ratio	(^{234}U/^{232}Th) activity ratio	(^{238}U/^{232}Th) activity ratio	Age (ka) Uncorrected	Age* (ka) Corrected
MHAOS-01	Unit *I*-4 Stalagmite	TIMS	13.837 ± 0.078	897.284 ± 6.703	5.033 ± 0.0287	0.047 ± 0.002	11.023 ± 0.354	237.198 ± 2.517	47.130 ± 0.441	5.148 ± 0.056	
BCW04-01	Unit *I*-3 Stalactite	TIMS	17.436 ± 0.119	265.108 ± 1.896	4.903 ± 0.038	0.029 ± 0.001	28.383 ± 0.512	985.592 ± 11.301	201 ± 1.985	3.167 ± 0.056	
MHA02-M1	Unit *I*-1 Dripstone fraction	TIMS	11.091 ± 0.079	8.965 ± 0.072	3.786 ± 0.106	0.274 ± 0.019	3.921 ± 0.256	14.313 ±0.417	3.781 ± 0.040	33.476 ± 2.687	16.501 ± 1.749
MHA02-M1	Unit *I*-1 Diamicton fraction	α[1]	451.110 ± 3.307	764.798 ± 58.621	1.280 ± 0.050	0.953 ± 0.055	2.185 ± 0.202	8.696 ± 0.704	6.7922 ± 0.558		
MHA02-M7	Unit *I*-1 Dripstone fraction	TIMS	55.844 ± 0.303	11.885 ± 0.094	3.081 ± 0.033	0.159 ± 0.006	7.014 ± 0.250	44.239 ± 0.616	14.36 ± 0.138	18.43 ± 0.708	14.09 ± 1.154
MHA02-M7	Unit *I*-1 Diamicton fraction	α[1]	540.255 ± 0.013	987.098 ± 67.485	1.201 ± 0.045	0.902 ± 0.051	1.799 ± 0.153	12.79 ± 0.933	10.656 ± 0.789		

* The dripstone subsamples were corrected for the detrital contribution for U and Th isotopes using the measured values of U and Th in the diamicton.

[1]Alpha spectrometry

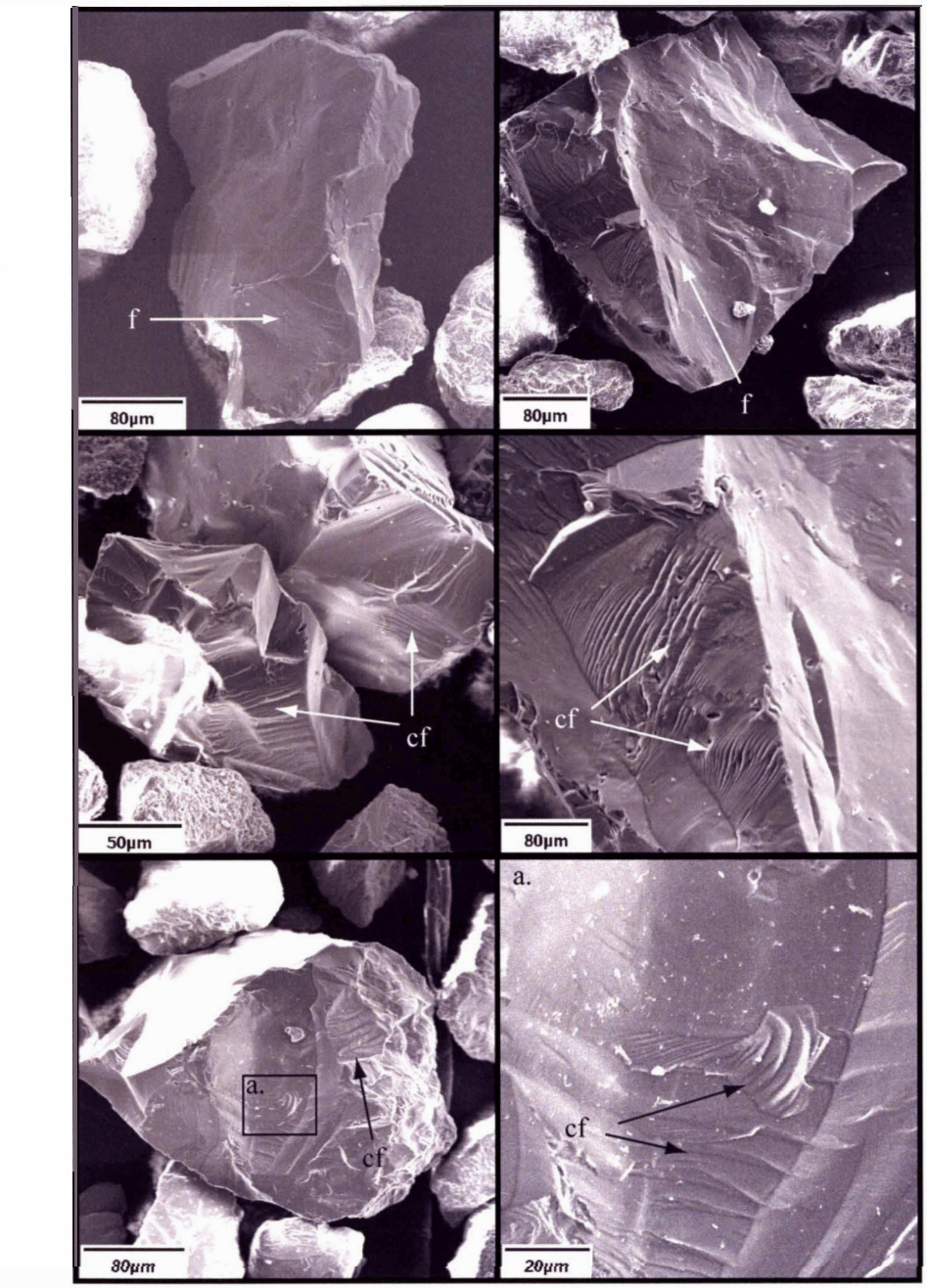

Figure 3.7. SEM images of quartz and feldspar grains from Unit *I*-1. Note the conchoidal fracturing (f), crushing features (cf) and angular surface textures.

Unit *I*-1 records ice-free conditions from >18.0 to 16.3 ka BP (Table 3.1, 3.2; Figure 3.6). It represents either the paleo-floor of the cave or sediments from the floor of the cave that were remobilized during late Wisconsinan glaciation. The range in ages as well as bone colours and weathering, in the lower and upper parts of the unit indicates some mixing either through bioturbation or colluviation. We favour colluviation as the explanation: bone concentrations do not decrease with depth; no biogenic structures were observed; and faint stratification is present. Quartz grains show little sign of transport. Although some of the grains are sub-angular with slight rounding of the edges, they bear none of the common characteristics of grains derived from subaqueous or aeolian environments, notably rounding and smooth or frosted surfaces (e.g., Krinsley and Doornkamp, 1973, Van Hoesen and Orndorff, 2004). This sediment may have been emplaced by a previous glaciation close to the entrance to the cave. With the onset of late Wisconsinan glaciation, the sediment and the bones on its surface could have been transported a short distance into the cave by means of sediment gravity flows. This hypothesis explains the crude stratification and fine-grained matrix of the upper 15 cm of the unit, and is supported by the intact character of many of the bones.

Unit *I*-2

Unit *I*-2 is 2 m thick (cumulative thickness of 3.3 m) and well stratified, comprising predominantly thinly bedded to finely laminated silt and clay, with interbeds of massive and convoluted clay and rare sand partings (Figure 3.5). Its lower contact drapes the irregular surface of Unit *I*-1 and contains isolated larger clasts. The grain size of samples average 83% clay. The stratification varies from a massive blue-grey clay approximately 18 cm thick, to light brown laminations of less than 1 mm. Individual laminations are dominantly normal graded, with some reverse grading, and locally they display evidence of soft-sediment deformation. This unit

contains numerous faults along with a large fault oriented parallel to that of the cave bedrock, and two ice-wedge pseudomorphs.

Unit *I*-2 can be divided into two packages of fine-grained sediment, a lower one 25 cm thick and dominated by massive clay, and the other comprising mainly very pale brown interlaminated clay and silt. The lower 25 cm of Unit *I*-2 consists of massive, dark grey clay that irregularly drapes the clasts at the top of Unit *I*-1. Two distinctive, bluish-black clay layers, each approximately 1 to 2 cm thick, are in sharp contact with massive clay in the lowest 15 cm of the subunit. These two layers are approximately 50% clay and 32% very fine silt (modal diameter 4.59 μm). The massive clay comprise approximately 92% clay-sized material; its modal diameter is 0.64 μm. Zones of diffuse, discontinuous laminations are noted in Unit *I*-2 but they are more weakly expressed than in the rest of the unit. A fault plane, which trends approximately parallel to the cave wall, cuts the unit. The fault plane strikes roughly north-south and displays slickensides.

The interlaminated fine silt and clay subunit, consists of pale brown to bluish grey laminations and lesser dark grey laminae <1 mm in thickness. Some laminations display reddish-brown mottling. There are visible microscale deformation features, such as flame structures, rare rip-up clasts, and small to large-scale convolute bedding. There is no evidence of ripples or other large-scale physical structures. Some laminations appear to grade from light grey to dark grey, terminating at a sharp contact and a return to light grey colours. This was confirmed from thin-section analysis, which showed a recurring pattern of normally graded laminations, light brown in colour, characterised by fine silt or clay passing upward into dark grey clay and capped by a sharp upper contact. This subunit contains numerous normal faults with displacements on the order of a few centimetres to tens of centimetres, most evident in the upper portion of the unit, within a package of distinct dark grey and dark brown laminations (Figure 3.5). In general, these faults dip toward the back of the cave and their dips and displacements decrease down-fault.

Unit *I*-2 contains two ice-wedge pseudomorph structures occurring at the same horizon. The larger of the two structures is in the lower 90 cm of the section (Figure 3.8). The larger ice-wedge pseudomorph tapers sharply from 110 cm wide at the top to 4 cm wide near the base where it terminates at the contact with Unit *I*-1. Its margins with adjacent, normally faulted, laminated silt and clay are sharp. The lower half of the wedge is dominantly light brown fine-grained sand and silt with minor proportions of contorted laminated fines. Thin (1 to 2 mm) fractures, comprising light brown fine-grained sand extend outward and downward, up to 6 cm from this zone. Near the base of the wedge is a vertical lens of medium-grained sand that is 3-4 cm wide at the contact with Unit *I*-1, and gradually narrows upward, terminating 35 cm from the base. Irregular lenses of similar fine-grained sand are present approximately 10 cm higher in the section. Above this, the light brown fine-grained sandy silt is increasingly mixed with fine-grained materials from adjacent to the wedge. These mixed beds are convoluted and brecciated, but include competent, normally fault-bounded blocks. The lower most 20 cm of laminated sediments that drape the wedge display a graben-like structure. The other wedge feature was similar but smaller and was not described in detail.

Three samples of Unit *I*-2 were analysed by X-Ray diffraction. Sample M3 came from the lower, massive grey clay; sample GS-9 is very dark grayish brown clay; and sample GS-8 is from one of the bluish black beds. The samples yielded similar diffraction patterns, with peaks of quartz, feldspar, and chlorite or corrensite. Samples GS-8 and GS-9 also contained calcite as well (Figure 3.9).

Loss-on-ignition analysis show low amounts of organic and inorganic carbon. Loss of organic carbon ranges from approximately 7 to 2 %, with an overall decline through the section. The inorganic carbon values were generally <1%, but were as high as 2% in the lower most 20 cm of the unit.

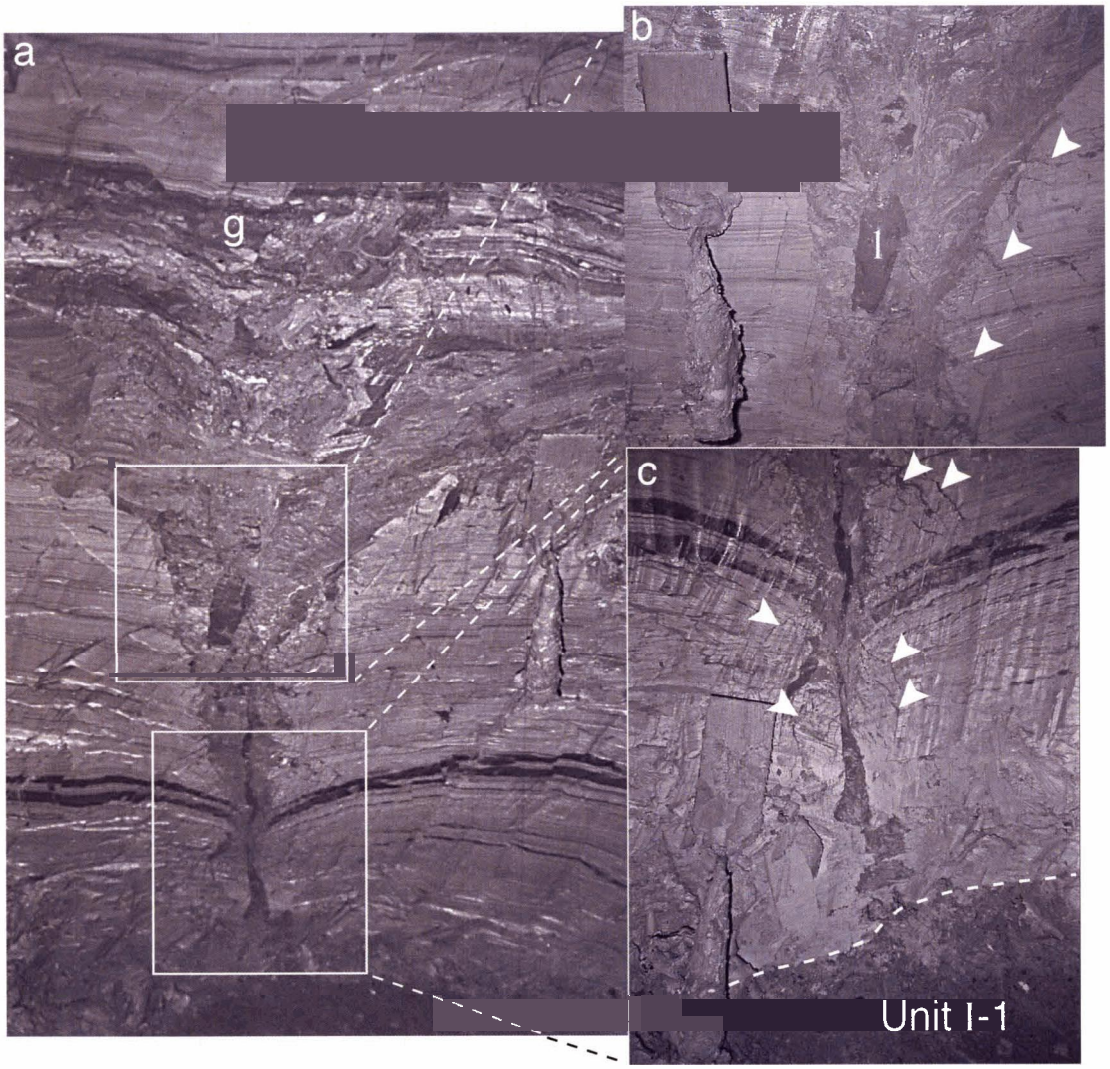

Figure 3.8. Large ice-wedge pseudomorph in Unit *I*-2 (trowel in all views is 26 cm). a. A graben-like structure is present in sediments draping the wedge feature (g); b. middle portion of the wedge with a mix of fine-grained sediments, from Unit *I*-2 and silty fine sand (1). Thin fractures of fine-grained sand extend outward and downward from the margin of the wedge (arrowed); c. lower portion of wedge and the lower contact with the diamicton of Unit *I*-1. A vertical dyke of fine-grained sand extends from the contact to the top of the view. Thick dark clay layers dip downward adjacent to the wedge. Thin fractures of fine-grained sand extend outward and downward from the margin of the wedge (arrowed).

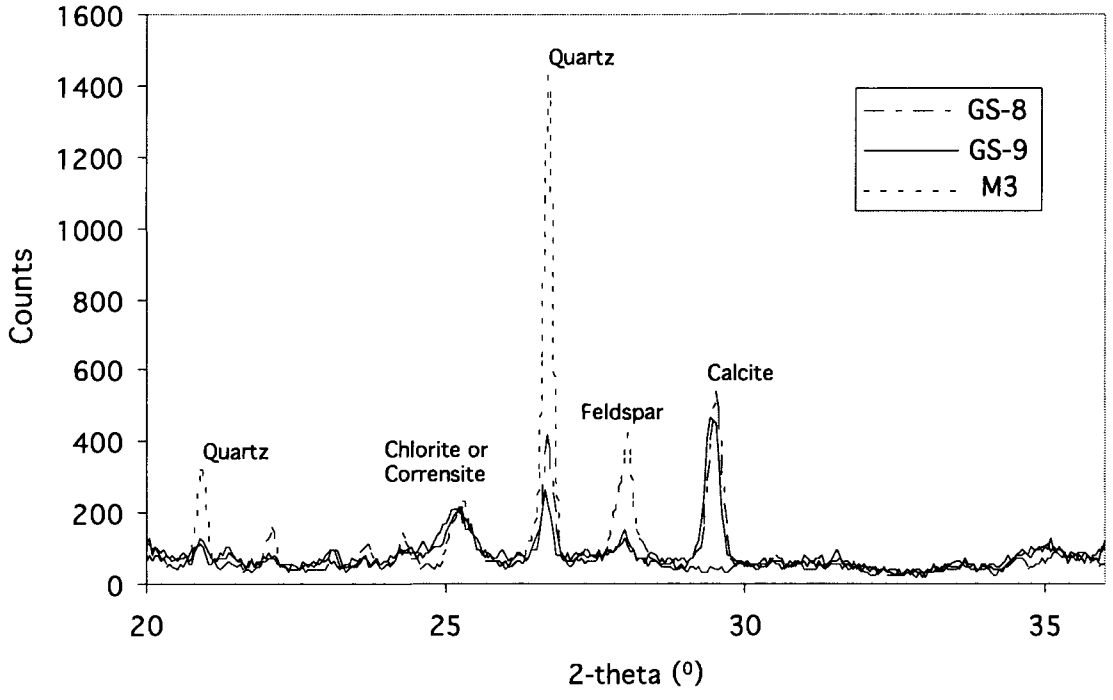

Figure 3.9. XRD spectra of clay samples from Unit *I*-2.

Unit *I*-2 has extremely high levels of remnant magnetization. Values of 1 to 6 A/m are the highest sediment values measured in the GSC-Pacific paleomagnetism laboratory (Enkin, personal communication 2002) and are normally found only at outcrops hit by lightning. Patterns of declination and inclination are typical of a few hundred or thousands years of geomagnetic secular variation.

The laminated silt and clay of Unit *I*-2 represent deposition from suspension under very low energy subaqueous conditions, such as a sub-glacial lake, as indicated by the clay-rich nature of the sediment, the strong remnant magnetization, the clay mineralogy, and the detailed sedimentology. Grain-size analysis shows little difference between samples and that they all have high amounts of clay. Thin-section analysis shows no current-generated structures (consistent with deposition under calm conditions). The sediment is predominantly quartz and feldspar; the lack of clay minerals suggests that the sediment is glaciogenic rock flour. Low organic and inorganic carbon values strengthen the argument for glacial deposition. The higher values of carbon in the lower most 20 cm are likely due to the larger amounts of carbon in the system during the initial stages of glaciation, as the glaciers overrode soils and vegetation. The origin of the different coloured laminations is unclear, as they do not appear to reflect differences in grain size or clay mineralogy.

The wedge-shaped features are interpreted to represent ice-wedge casts based on their characteristic tapering shapes, the thin fractures extending out and down from the wedges, the associated normal faulting in adjacent sediments, and the variable character of the material filling the features. This interpretation suggests that the subglacial lake drained and sediments were subaerially exposed. Two scenarios are proposed to explain this: (1) oscillation of the ice front; and (2) changes in subglacial drainage. We favour the first explanation (see Chapter Four).

Normal faulting of material draping the larger structure indicates the melting of at least a portion of the ice-wedge after burial.

The fault that parallels the cave wall and cuts the bulk of Unit *I*-2 may record reactivation, following deglaciation, of the fault that formed the cave. Reactivation could be caused by glacio-isostatic adjustments or may have occurred during one or more earthquakes. The smaller normal faults may either be related to the same event, or the result of differential compaction of the sediments. The dykes of medium-grained sand in the lower part of the larger ice-wedge cast may have been injected during liquefaction of the underlying diamicton.

Unit *I*-3

Overall Unit *I*-3 consists of, massive, oxidized clays with some convolute bedding (Figure 3.4). This forms the floor of the interior cave chamber. The unit has a sharp lower contact with the laminated silt and clay of Unit *I*-2. A partially disarticulated skeleton of a mountain goat was found down to a depth of approximately 30 cm in Unit *I*-3, along with associated dripstone and charcoal fragments. The mountain goat and an overlying charcoal fragment yielded ages of 12.3 and 9.5 ka BP, respectively (Table 3.1, Figure 3.4).

Unit *I*-3 is interpreted to be a post-glacial deposit, formed as a result of redeposition of the upper part of Unit *I*-2 in ponded water. The sediments are oxidised due to periodic drying of the cave floor. Dripstone fragments and soda straws in Unit *I*-3 have fallen from the roof of the cave.

Unit *I*-4

Unit *I*-4 consists of modern cave sediments, including stalagmites, stalactites, other flowstones, and rubble at the entrance to the chamber. Several stalagmites in this unit were

forming around the area of the excavation. U-series analyses from one of the stalagmites as well as from a stalagtite fragment from the base of the unit yielded ages of 5.1 and 3.2 ka BP, respectively (Table 3.2). The base of the dripstone unit has a lower sharp contact with the underlying oxidized clay of Unit *I*-3.

Sediments of the cave entrance complex

Unit *E*-1

Unit *E*-1 is a matrix-supported diamicton that occurs at the base of the 5 m vertical section near the cave entrance (Figure 3.4). It is > 0.5 m thick and extends an unknown distance into the cave. The lower contact is not visible. The diamicton contains large subrounded to rounded boulders (the largest >1.5 m).The largest clasts consist of cave rock, whereas pebbles and cobbles are dominantly of exotic lithologies. The matrix comprises 88% coarse silt or finer sediment. Matrix sand grains are angular with conchoidal fractures. The matrix and surface of the deposit contains calcium carbonate.

Unit *E*-1 is interpreted to be till, emplaced by ice that blocked the cave entrance. Such a scenario would explain the presence of exotic clasts. The larger blocks of cave material were likely pushed ahead or incorporated into the ice. Conchoidally fractured, angular grains are similar in morphology to those in Unit *I*-1 (Figure 3.8). The presence of this ice and associated melt water would have allowed the cave to fill with water, and therefore the unit is likely correlative with the laminated silt and clay of Unit *I*-2.

Unit *E*-2

Unit *E*-2 is a clast-supported diamicton that forms the floor of the modern cave entrance. It comprises the upper 4 m of the vertical section at the cave entrance (Figure 3.4) and is exposed

at the surface in the outer cave complex as well. It has an irregular, sharp basal contact with Unit *E*-1. Unit *E*-2 largely comprises openwork angular cave-rock blocks, some more than 1.5 m across. Fine-grained sand and silt with rare bone form the matrix of the unit at the surface.

Unit *E*-2 is interpreted to be a post-glacial deposit, resulting from rock-fall from the roof of the cave. It is, therefore, probably correlative with the oxidised clays of Unit *I*-3 and the speleothems of Unit *I*-4. Since ice retreat, the roof of the cave has likely been subjected to freeze-thaw action. Seismic events may have also contributed to this accumulation, as the area is seismically active with extensive evidence for numerous earthquakes (Clague and Bobrowsky, 1990).

Faunal assemblage

More than 4000 bones were recovered from Unit *I*-1, and represent a diverse vertebrate fauna (Table 3.3). The fauna is interpreted to be indicative of the paleoenvironment near the cave between 18 ka and 16 ka BP. The assemblage is dominated by small mammals and birds. Mammals include three species of vole, a marten and an alpine marmot, but also contains larger fragments from at least one larger species, notably, a mountain goat. Various fish species are also documented throughout the sequence, as well as mussel and barnacle shells, which appear to be more common near the base of the interval.

Several mammal species suggest an open landscape. Among these mammals are three species extirpated from Vancouver Island and possibly an extinct species. Of the three voles, only Townsend's vole occurs on Vancouver Island today, principally in non-forested habitats from sea level to 1740 m (Nagorsen, 2004). The long-tailed vole ranges widely from wet meadows through shrub thickets to forests. The heather vole typically inhabits open coniferous forests, but also occurs in the alpine environment with marmots. The alpine marmot group is restricted to treeless

Table 3.3 Animal species from Port Eliza cave

Taxon	*Common Name*
Nonglacial Fauna	
Fish	
Onchorhynchus sp.	salmon
Oncorhynchus ?clarkii	?Cutthroat Trout
Gasterosteus sp., cf. *G. aculeatus*	threespine stickleback
Hexagrammidae, indet.	greenling
Theragra chalcogramma	pollock
Pleuronectiformes, indet.	flatfish
Hemilepidotus sp.	Irish lord
?Cottidae, indet.	?sculpin
Microgadus proximus	Tomcod
Amphibians	
Bufo boreas	western toad
Birds	
Gavia sp., cf. *G. stellata*	small loon (?red-throated)
Alcidae, indet.	small alcid
cf. *Phalacrocorax* sp.	cormorant
cf. *Anas* sp.	?small duck
cf. *Eremophila alpestris*	?horned lark
Passerculus sandwichensis	savannah sparrow
additional bird species	
Mammals	
Microtus townsendii	Townsend's vole
M. longicaudus	long-tailed vole
Phenacomys intermedius	heather vole
Marmota sp., cf. *M. caligata*	marmot, alpine group
Martes americana ssp., cf. *M. a. nobilis*	large (?noble) marten
Oreamnos americanus	mountain goat
Carnivora, indet.	?canid (tooth mark evidence)
Molluscs	
Mytilus sp.	mussel
Balanus sp.	barnacle
Postglacial Fauna	
Mammals	
Peromyscus sp.	mouse
Oreamnos americanus	mountain goat

habitats. The modern Vancouver Island marmot constitutes the most endangered mammal in Canada, and is restricted to small areas of grass-forbs meadows above 700 m above sea level (Bryant and Janz, 1996; Nagorsen *et al.,* 1996). Mountain goats similarly favour meadows and cliffs in the alpine zone, and though they occurred on Vancouver Island after the LGM, were extirpated by the end of the Pleistocene likely because of habitat restriction (Nagorsen and Keddie, 2000).

The Port Eliza cave derived species that is most suggestive of forest conditions is the marten, which today is associated with dense coniferous forest. However, late Pleistocene marten remains in Beringia occur in settings interpreted to include taiga and steppe (Graham and Graham, 1994). The Port Eliza cave specimen is larger than the modern marten, and is similar in size to the extinct noble marten (*M. nobilis*) and modern marten on the Queen Charlotte Islands (*M. a. nesophila*). Taxonomy of the noble marten is unclear. Some authors view it as a subspecies of *Martes americanus* (Youngman and Schueler, 1991), while others interpreting it as a separate species with wide habitat tolerance. Grayson (1984, and pers. comm., 2003) reported *M. nobilis* from Holocene cave deposits in Nevada and Idaho that lacked boreal faunal elements. Consequently, the marten remains cannot be taken as diagnostic of boreal conditions. The passerine birds (e.g., savannah sparrow and possible horned lark) are consistent with open conditions. On balance, the fauna is interpreted to indicate an open landscape, possibly with some isolated stands of trees.

Fish remains indicate that the sea was close to the cave entrance, and represent a varied fauna capable of supporting terrestrial predators and scavengers. With the exception of salmon (*Oncorhynchus sp.*) and trout, the taxa are completely marine (i.e., greenling, pollock, flatfish, Irish lord, Tomcod and sculpin), suggesting that the shoreline was close enough for predators to bring such material back to the cave. The presence of abundant shell fragments, including

mussels and barnacles, further confirms this supposition. Salmon and trout probably also represent capture or scavenging from local freshwater streams.

Pollen and spores

Pollen and spores were recovered only from units *I*-1 and *I*-3 (Figure 3.10). Pollen abundances are low, with scarcely 100 palynomorphs in several of the samples. All samples are dominated (>70%) by non-arboreal pollen (NAP). NAP consists mainly of grasses and *Selaginella,* with lesser amounts of Asteraceae, Apiaceae (mostly *Heracleum lanatum* - cow parsnip) and *Campanula* (harebel). The deepest sample in Unit *I*-1 has abundant Cyperaceae (sedges), and the highest sample in Unit *I*-3 contains relatively abundant Ericaceae (heath). Arboreal pollen (AP) consist mainly of *Pinus* (pine) and *Tsuga heterophylla* (western hemlock).

The palynological assemblages indicate open landscapes at the time of deposition of Units *I*-1 and *I*-3. No modern samples from the region, not even those from moss polsters, yield such high NAP values that are dominated by the taxa identified in this study (Hebda, 1983; Hebda and Allen, 1993; Allen *et al.,* 1999 and references therein). The abundance of grasses, Caryophyllaceae (pink family) and *Selaginella* (a diminutive spikemoss) indicates a landscape covered largely in low-growing, herbaceous species. Like *S. densa* or *S. wallacei,* or even *Campanula* (harebell), the *Selaginella* spore type is a likely indicator of dry conditions. Notable are the low values of pollen derived from shrubs, such as *Alnus* (alder) and *Salix* (willow), suggesting that few woody plants grew in the area during this interval. Samples with abundant Cyperaceae, near the base of Unit *I*-1 and the top of Unit *I*-3 reflect the widespread occurrence of moister communities in the region.

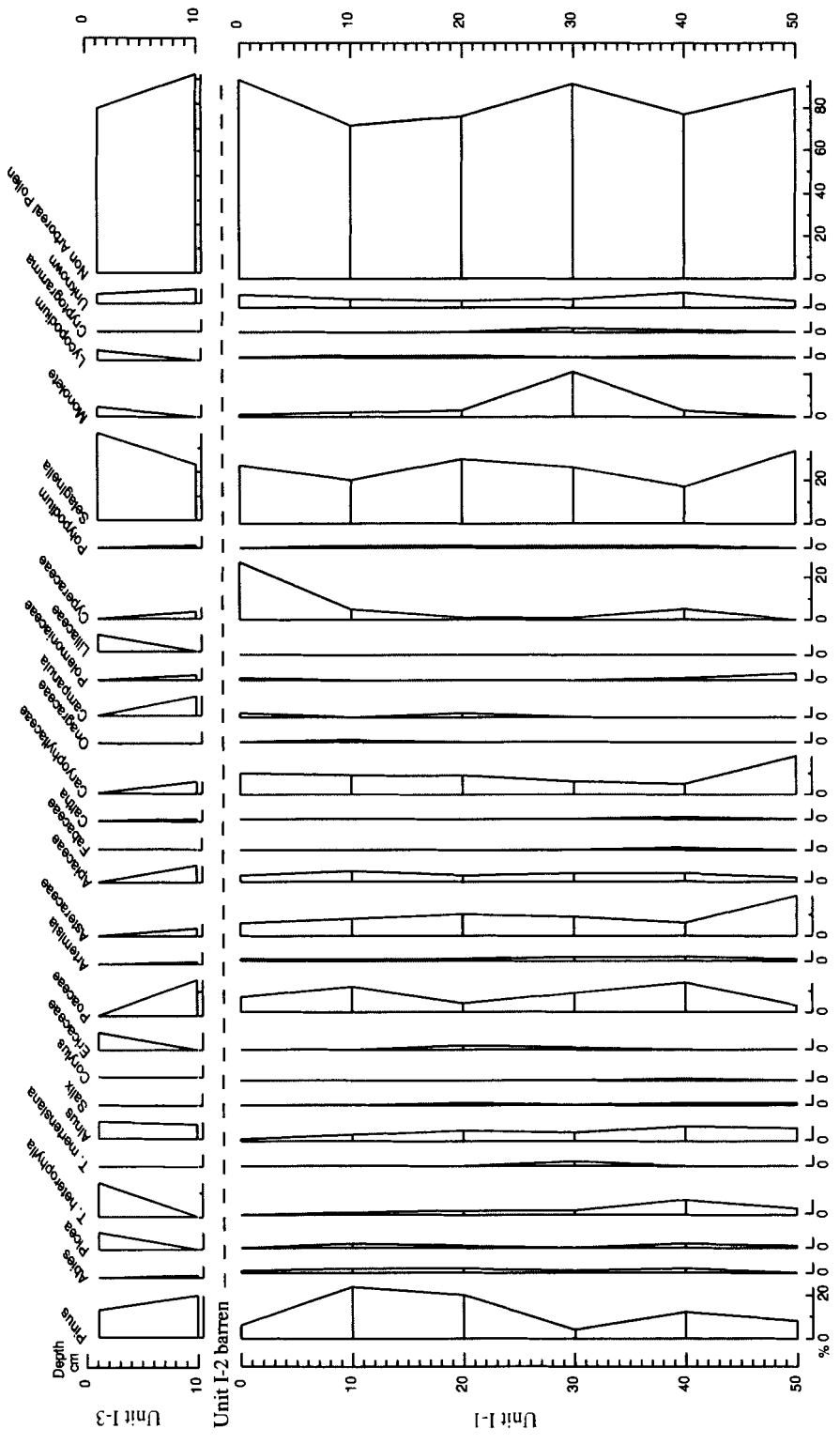

Figure 3.10. Pollen from Unit *I*-1 and Unit *I*-3.

Paleoenvironmental reconstruction

The faunal and floral assemblages of Unit *I*-1 provide a picture of the pre-LGM environment 18 to 16 ka BP. The dominantly herbaceous landscape suggests a cold dry climate. The arboreal pollen, mainly pine, can be accounted for by long-distance (aeolian) dispersal. The occurrence of scrubby vegetative trees, however, should not be ruled out as pine is present at Tofino *ca.* 16.7 ka BP (Figure 3.1, Blaise *et al.,* 1990). The landscape supported a wide variety of small mammals and birds, and at least one larger species (e.g., mountain goat). Local streams contained trout. The sea was close to the cave entrance and contained salmon and other shallow-water fish, as well as shellfish. The fact that the sea was close to the cave at a time when eustatic sea level would have placed the shoreline approximately 15 km away points to significant isostatic depression. Thus, Vancouver Island supported large glaciers that would likely have been visible from the shore.

The cold dry environment recorded at Port Eliza has not been reported in other sediments of the region during the pre-LGM interval. Unit *I*-1 assemblages span a period contemporaneous with, or slightly younger than sediments of the Port Moody Interstade of the Fraser Lowland (Figures 3.1, 3.2), yet the pollen assemblages of the two sites are not at all similar. The Fraser Lowland supported an open spruce-fir forest (Hicock *et al.,* 1982); whereas the Port Eliza area was cold and probably possessed only scattered trees. If the two sites are contemporaneous, a steep climatic gradient existed between them. One would expect, however, a more temperate climate at Port Eliza than in the Fraser Lowland, because the cave is much nearer the open Pacific Ocean. Based on the mixed palynological assemblages, indicated by the range in radiocarbon ages, the pollen spectra could reflect conditions near to *ca.* 16 ka BP, a time closer to the LGM and reflecting pronounced cooling or drying after the Port Moody Interstade. Vegetation on the

Queen Charlotte Islands *ca.* 15 ka BP consisted of tree-less tundra dominated by grasses, sedges, *Caryophyllaceae*, and other herbaceous plants (Mathewes, 1989).

The laminated silt and clay (Unit *I*-2) and the diamicton (Unit E-1) at the entrance to the cave, mark local glacier occupation after 16 ka BP. XRD and SEM data indicate a glacial source for these sediments. Paleomagnetic data point to a realtively long period of deposition in still water. The observations confirm that the outer coast of Vancouver Island was glaciated during the late Wisconsinan. The bounding dates on Unit *I*-2 constrain time of local glaciation.

The radiocarbon age on the mountain goat in Unit *I*-3 provides a minimum age for local deglaciation, and is similar to ages yielded by bones of two other mountain goats (12.3 and 12.5 ka BP) from northern Vancouver Island (Nagorsen and Keddie, 2000). Older radiocarbon ages (13.1 and 13.6 ka BP) based on bulk sediment from lakes, suggest deglaciation could have been earlier (Hebda, 1983). Pollen in Unit *I*-3 is similar to Unit *I*-1 and suggests open parkland with dry herbaceous shrub cover and rare stands of pine and alder. Mountain goats reached northern Vancouver Island by 12.5 ka BP, either by migration from refugia to the north on the now submerged continental shelf (Hetherington *et al.,* 2004) or from the south (Nagorsen and Keddie, 2000).

Implications for human migration

Data presented here provides important clues into the viability of the coastal migration hypothesis. The oldest known British Columbia coastal archaeological sites are Namu, on the central mainland coast alongside Fitzhugh Sound, dated at 9.7 ka BP (Carlson, 1996a, b) and at Hunter Island, 20 km to the west dated to 9.9 ka BP (Cannon, 2000*)*. The oldest securely dated archaeological site on Haida Gwaii is Kilgii Gwaay, dated to 9.4 ka BP (Fedje *et al.,* 2001) and in a karst cave on Prince of Wales Island, southeastern Alaska, a culturally modified, terrestrial

mammal bone yielded an age of 10.3 ka BP (Fedje *et al.*, 2004). Isotopic studies of human remains from the same site indicate a dominantly marine diet at 9.2 ka BP. Older post-glacial human occupation sites are likely to be found in all of these areas, especially on Prince of Wales Island where trace element analysis of obsidian artifacts indicates that an extensive trade network had already been established by 9 to 10 ka BP (Fedje *et al.*, 2004). People were present to the north, in eastern Beringia, at 12 ka BP and perhaps earlier (Cinq-Mars, 1979; Cinq-Mars and Morlan, 1999; Hamilton and Goebel, 1999; Dixon, 1999). South of British Columbia, the earliest well-dated human occupation site is 11.4 ka BP at Cooper's Ferry in the lower Salmon River valley, Idaho. A cache pit extending down from this level gave ages of 11.4 and 12.0 ka BP and contained four stemmed projectile points (Davis and Sisson, 1998). Several other sites of the stemmed point tradition in the Great Basin and Snake River Plain appear to be of the same age (Bryan and Tuohy 1999). A stemmed point associated with the youngest Glacier Peak tephra (*ca.* 11. 25 ka BP) was recovered at Pilcher Creek, northeast Oregon (Brauner, 1985) and a cache of Clovis fluted projectile points (one resting on the surface of the tephra) at the Richey-Roberts site near Wenatchee, Washington (Mehringer and Foit, 1990). Each occurrence is interpreted to immediately postdate the ashfall event. The Indian Sands site on the Oregon coast includes a human occupation site associated with a paleosol that has been dated to 10.4 ka BP (Davis, 2003; Davis *et al.*, 2004).

Dixon (1999) has argued that North America was first colonized by people who used watercraft to travel down the west coast *ca.* 13.5 ka BP, supporting the coastal migration hypothesis of Fladmark (1983). An initial criticism of the coastal migration theory was that much of the route was barred by the extensive Cordilleran Ice Sheet, which had advanced to the shelf edge (Prest, 1969). However, this study and other recent work (Blaise *et al.*, 1990; Mann and Peteet, 1994; Heaton *et al.*, 1996; Josenhans *et al.*, 1997; Barrie and Conway, 1999; Fedje and

Josenhans, 2000; Hetherington *et al.*, 2003, 2004) indicate that the LGM was diachronous and not as extensive and long lived as once thought, allowing the possibility of human migration.

Evidence suggests that glaciers in southern Alaskan coastal areas were retreating by or before 16 ka BP, following an earlier expansion at 23 ka BP (Mann and Peteet, 1994). Data from Port Eliza cave show that the LGM on northern Vancouver Island occurred after *ca.* 16 ka BP, raising the possibility that there was a brief window of opportunity for migration along an ice-free Northwest Coast immediately prior to 16 ka BP. Refugia likely existed in southeast Alaska, supporting terrestrial mammals as well as seals (Heaton and Grady, 2003). Glaciers on Haida Gwaii (Queen Charlotte Islands) were at their maximum prior to 16 ka BP and were retreating by 15 ka BP (Clague *et al.*, 2004). Ice-free areas, however, may have existed along the west coast of Haidai Gwai and on the now-submerged continental shelf (Fedje *et al.*, 2004; Ramsey *et al*, 2004). The presence of brown bear at 14.3 ka BP (Ramsey *et al.,* 2004) implies adjacent coastal refugia, because migration routes from the south along Vancouver Island would have been blocked by glaciers. Early migrants would still have had to deal with extensive sea ice (Brigham-Grette *et al.*, 2004) and have to have skirted major ice lobes along the way (e.g., in Hecate Strait), but Dixon's (1999) strong argument for use of watercraft by the earliest colonising populations applies here; if, as he argues, they were using water craft by 13.5 ka BP, much the same situation could have prevailed 2500 years earlier.

Humans would have found a hospitable environment on the west coast of Vancouver Island before 16 ka BP. The fauna appears to have been dominated by small species, the presence of mountain goat indicates an environment also amenable to ungulates and, by extension, capable of supporting small human populations. The diverse assemblage of fish material at Port Eliza cave signifies a nearby, rich marine environment. The presence of salmon indicates seasonal anadromous fish runs in local streams. There were also likely sea bird colonies along the coast.

Marine and terrestrial resources although perhaps less abundant than today, could have supported humans.

Conclusion

Port Eliza cave deposits provide multiple lines of evidence on the character of the LGM on the west coast of Vancouver Island. The site was glaciated only after 16 ka BP and could have supported humans before this date. The presence of a diverse fauna and flora near the cave shows that food resources were adequate to support humans. Palynological data indicates a cold, dry, open landscape. Mountain goat fossils show that the environment was capable of sustaining large herbivores. Fish species such as salmon would have offered an important source of protein for potential human migrants.

The onset of glaciation is signalled by deposition of laminated silt and clay in Port Eliza cave. Deglaciation occurred before 12.5 ka BP. The implication, therefore, is that for this section of the coastal migration route, the terrestrial environment would have been unavailable to humans for no more than 3000 years.

Findings at Port Eliza Cave are thus of importance to the ones of human entry into the New World. It is clear that the west-coast was blocked by Cordilleran ice only briefly and that the glacial maximum may have been diachronous in different areas. If the humans who occupied Monte Verde, Chile 12.5 ka BP, came from northeast Asia, there are three possible scenarios for west-coast travel: after 13 ka BP, shortly before 16 ka BP, or well before to the LGM (Madsen, 2004). The post-13 ka BP scenario would have required rapid southward movement, which is plausible, given the likelihood that watercraft could be used for the journey. The pre-16 ka BP and earlier scenarios allow several millennia or more for people to reach Chile. Coastal sites from such an early southward movement either would have been overridden by ice at the LGM,

destroyed by wave action, or submerged by the sea. Even south of the Cordilleran Ice Sheet, any record of the movement of marine-adapted peoples would suffer from the last two problems. Discussions of the possible availability of watercraft and associated technologies at 16 or 13 ka BP is inconsequential given that people apparently migrated across open ocean to Australia at least 38 ka BP and perhaps earlier (Allen and Holloway, 1995; Mulvaney and Kamminga, 1999). What is needed now is a detailed reconstruction and summary of the coastal paleogeography from Alaska to Washington 17 to 16 ka BP, a time once ignored as icebound and inapplicable to the question of human migration history.

CHAPTER FOUR

A RECORD OF LATE WISCONSINAN GLACIATION IN FINE-GRAINED SEDIMENTS, PORT ELIZA CAVE, CANADA

Introduction

Port Eliza Cave, on the west coast of Vancouver Island, preserves a detailed record of nonglacial, glacial and post-glacial paleoenvironments of the Fraser Glaciation (Ward *et al.*, 2003; Al-Suwaidi *et al.*, in press). This paper focuses on distinctive fine-grained, well-laminated sediments within the cave (Figure 4.1), deposited when ice covered the outer coast of Vancouver Island. A major problem in the study of proximal glacial sediments such as these is the lack of internal chronological control, due to the scarcity of datable material. Paleomagnetism has been successfully used in the study of cave sediments in Norway for dating and correlating between cave sites (e.g., Valen *et al.*, 1995, 1996; Mangerud *et al.*, 2003). Here, I present the results of thin section, carbon, and paleomagnetic analysis on a sequence of fine-grained sediments in Port Eliza cave. The objectives are to elucidate the character and timing of glaciation on the west coast of Vancouver Island, present a record of late Wisconsinan secular variation for the area between *ca.* 16 and 13 ka BP, and discuss the unique paleomagnetic properties of these sediments.

Sediments

The sediments of the "interior cave complex" consist of nonglacial (*I*-1), glacial (*I*-2) and post-glacial (*I*-3, *I*-4) units (Figure 4.1). Unit *I*-1 is an unsorted, matrix-supported diamicton, that was excavated to a depth of approximately 80 cm (see Chapter Three, Table 3.1). It contains bone

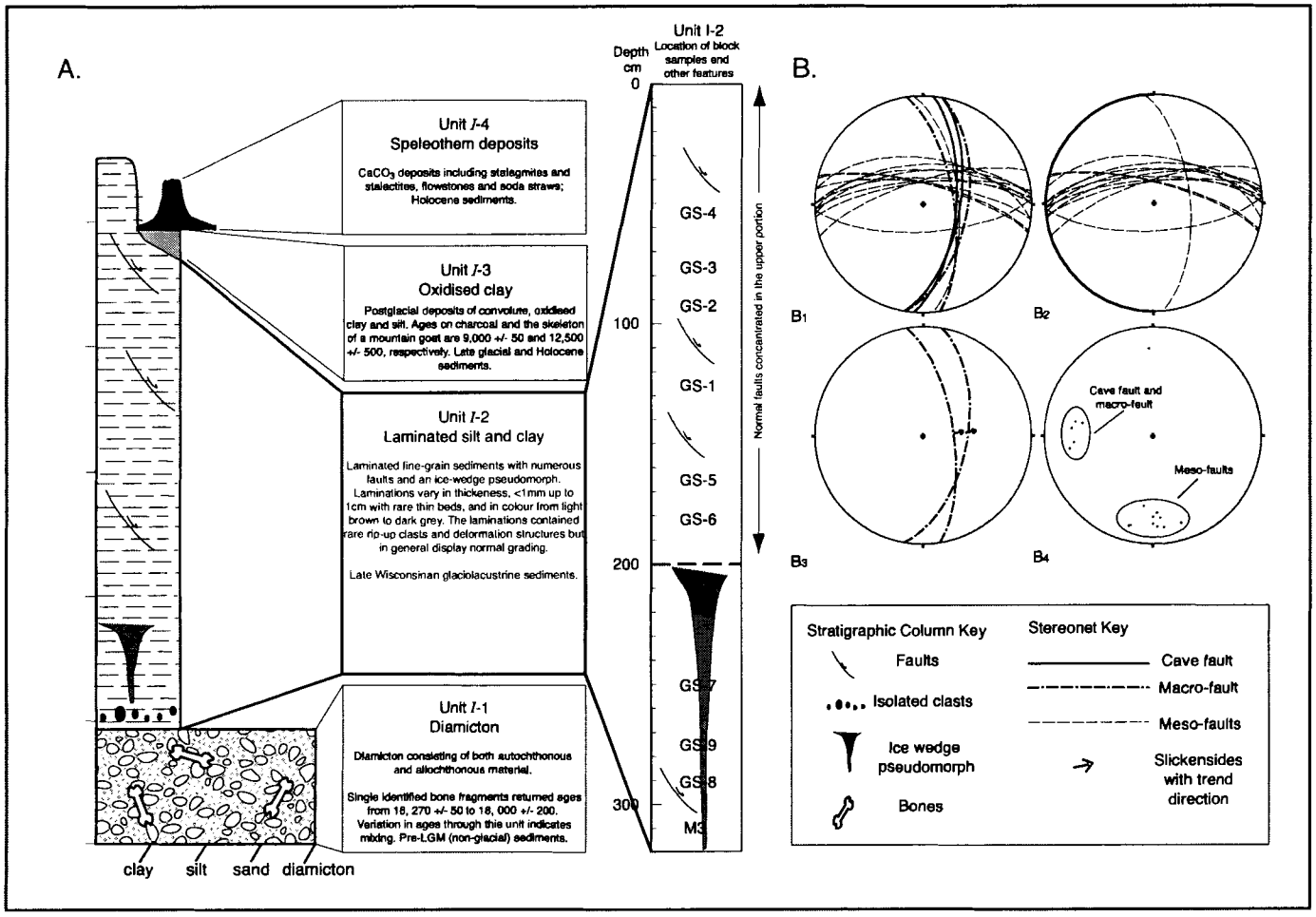

Figure 4.1. A. Summary of sediments of the interior cave complex with a focus on the sediments of Unit *I*-2; B. Stereoplots of faults in Unit *I*-2; B1, all the faults measured with respect to the main cave fault; B2, normal faults measure in the upper portion of Unit *I*-2; B3, faults measured near the base of Unit *I*-2; B4, poles of faults showing two populations.

material radiocarbon dated to between 18 and 16 ka BP, striated clasts, and dripstone fragments. Unit *I*-2 comprises thinly bedded to finely laminated silt and clay with interbeds of massive and convolute bedded clay with rare sand laminae. This unit has a cumulative thickness of 3.2 m (~2 m in section), two populations of faults and two ice-wedge pseudomorph structures interpreted to be ice-wedge casts. Unit *I*-3 consists of massive, oxidized clay with some convolute bedding, dripstone fragments, the bones of a mountain goat, and charcoal. The mountain goat skeletal material and the charcoal fragments returned ages of 12, 340 and 9, 540 BP, respectively (Table 3.1). Unit *I*-4 comprises modern cave sediments, including stalagmites, stalactites and other flowstones.

Faulting is common in Unit *I*-2 and they can be divided into two populations: a normal fault that cuts the entire unit and smaller listric faults (Figure 4.1). The large normal fault has an undulating surface striking 10° to 350° and dipping 55° to 70° east. Striations on the fault plane trend 86° and plunge 57° to 66°, indicating some obliquity to the movement. Laminations normal to the fault plane are lower on the eastern wall than on the western wall. Port Eliza cave formed along a fault that strikes 10° and dips 60° to the east, which is similar to the orientation of this fault (Figure 4.1). Twelve listric faults with displacements typically averaging 7.7 cm (max. 13.5 cm, min. 1.2 cm) were measured, and they have a general east-west strike (average 260°) and a northerly dip direction (average 70°).

The faults are post-depositional, having formed after consolidation of the unit. The similar orientations of the large normal fault and the cave fault suggest that the two are genetically related, and that the latter was reactivated. The listric nature of the meso-scale faults suggests that extension of Unit *I*-2 occurred. The relationship between the larger fault and the meso-scale faults is not clear. No cross-cutting relationships were observed, making it difficult to determine the relative timing of the two structures. It is possible that they are conjugate faults

formed as the Unit *I*-2 readjusted to the movement on the cave fault. The structures likely record post-glacial tectonic activity, possibly related to readjustment caused by either isostatic rebound or earthquakes.

Thin section analysis

Six samples of Unit *I*-2 were mounted in resin for thin section analysis (Chapter Two). The most striking feature in thin sections is the normal grading of the laminations. Very fine sand or more commonly silt fines upward to clay, which in turn is sharply overlain by silt sized particles of the next lamination (Figure 4.2). This structure is common throughout the sampled slabs. It was also noted that the silt commonly is lighter in colour than the clay and many of the laminae contain interlaminations of silt within the clay zones (Figure 4.2 a, b). No current-generated structures were seen and there are only a few soft-sediment deformation structures (Figure 4.2 c). The lack of current-generated structures, fine grain size, and uniform normal grading of the laminations, suggest that the sediments were deposited from suspension settling. The rhythmicity of the laminations and the lack of obvious unconformities in Unit *I*-2, indicate continuous sedimentation. These sedimentological observations are consistent with annual or sub-annual couplets. Rhythmites are dominant in the upper 100 cm of the section; thin sections from the lower part of the section showed fewer well-developed couplets and slightly coarser sediment (Figure 4.2 g, h).

Crystals of an iron mineral appear opaque in thin section (Figure 4.2 f). In Some cases the crystals had a dendritic or botryoidal habit. Some of the crystals display zonation, with a reddish oxidised zone surounding opaque cores. The crystals are commonly concentrated along fine-grained sand horizons. These are most common in sample GS-6, taken from roughly 200 cm depth in Unit *I*-2. The crystals are interpreted to be detrital magnetite; the reddish zones are

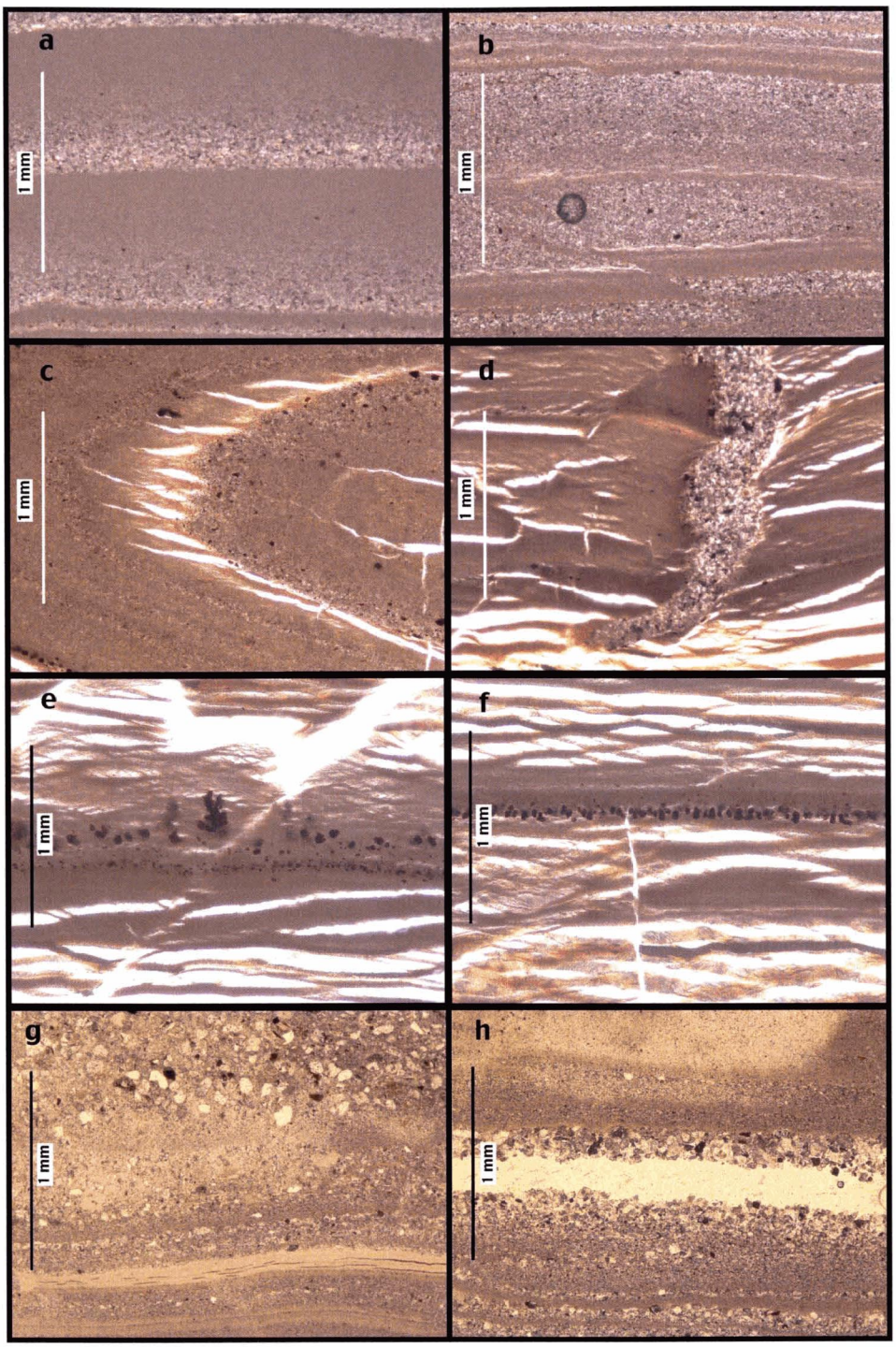

Figure 4.2. Thin sections of Unit *I*-2 showing: a. well-defined laminations, fining upward from fine-grained sand to clay; b. laminations and interlaminations showing possible sub-annual deposition; c. soft-sediment deformation in the form of folded laminae; d. injection of fine-grained sand into laminated silt and clay due to penecontemporaneous deformation; e. authigenic crystals of magnetite, displaying a botryoidal habit and cross-laminations; f. authigenic crystals of magnetite concentrated along a horizon of silt; g. and h., coarser fine sand to sand grain-sized sediments noted in the lower ~ 100 cm of Unit *I*-2.

probably haematite. Grains extracted using a magnet were analysed by SEM-EDS and displayed a single peak in iron consistent with magnetite. Some of the crystals cross laminations, however, suggesting they are authigenic. Many of these authigenic crystals appeared to be concentrated along laminations and interlaminations of coarser material (very fine sand or silt as opposed to clay). One possibility is that the ground water accelerated the oxidation of pre-existing detrital grains. It is important to stress that these authigenic growths were rare and the majority of opaque minerals identified as magnetite appeared detrital in character.

Loss-on-ignition

Loss-on-ignition (LOI) analysis was carried out on block samples of Unit *I*-2 (Chapter Two). Samples were chosen to represent the range in colour, lamination and bed thicknesses (Figure 4.1; Appendix H). The block samples span about 126 cm of the 320 cm total measured thickness of Unit *I*-2. Gaps between blocks were filled with cylinders of sediment collected for paleomagnetic analysis. The typical sample interval was 2 cm, providing a high-resolution data set (Figure 4.3).

The samples have low organic and inorganic carbon contents, and average <5% and <2%, respectively. The lowest value of organic carbon is 1.9% about 50 cm below the top of the section (Figure 4.3). The highest value (14.3%) is from a sample just above the ice-wedge, 176 cm below the top of the unit. Higher values were also obtained from the thin dark grey beds of clay at 270-290 cm (7.7% and 7.6%). The lowest values of inorganic carbon occur at 58 cm (0.3%) and near the base of the unit at 310 cm (0.7%). The highest values of inorganic carbon are at 270-290 cm (3.6 and 6%) and 170-190cm (3%), the same interval that has the highest organic carbon values (Figure 4.3).

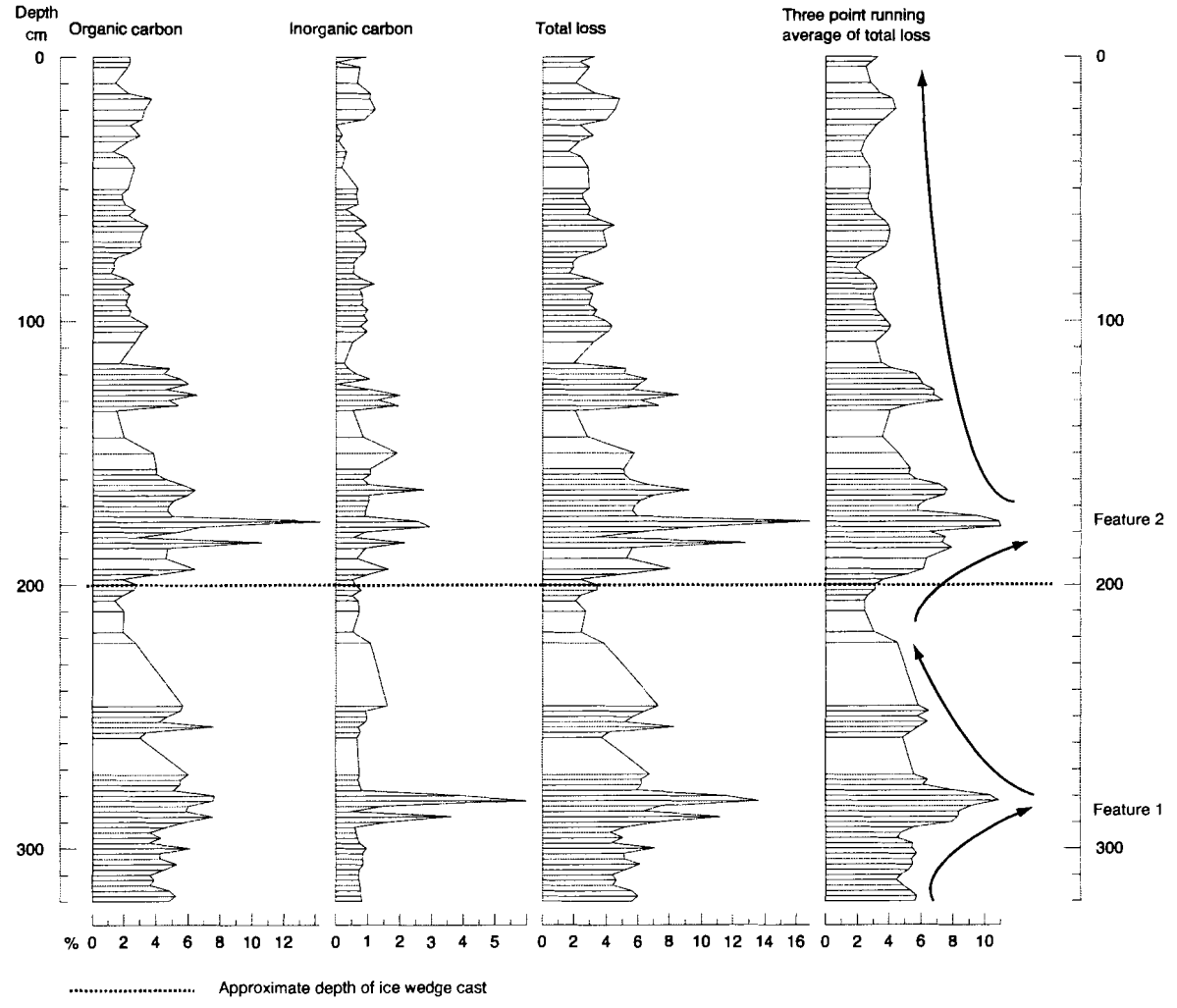

Figure 4.3. Loss-on-ignition resluts for Unit *I*-2. Note the peaks in organic and inorganic carbon (Features 1 and 2).

The relationship between glacial erosion and clastic sedimentary deposition in proglacial lakes has long been accepted (Karlén, 1976, 1981, 1998). Where glacial lakes have a negligible input of sediments from other sources, organic carbon content is a function of allochthonous production in the lake catchment and autochthonous production within the lake itself (Nesje *et al.*, 2000). The relationship of organic and inorganic carbon in subglacial lakes, such as Port Eliza, is not as clear. In a subglacial lake where the glacier is the only sediment source, organic productivity is negligible and carbon is only derived from plants and soils overrun by and incorporated into the advancing glacier. Thus, peaks in organic carbon likely reflect initial ice cover when larger amounts eroded soil and vegetation are still present in the basal debris layer of the glacier.

The low levels of organic carbon (<5%) in Unit *I*-2 are characteristic of a glacial environment. The higher values in the lower part of Unit *I*-2 may reflect initial glacial cover when higher levels of newly eroded organic carbon were present in the basal sediments of the glacier. The two peaks between 280 and 290 cm correspond with the two dark beds noted towards the base of the unit (Chapter Three). These beds were noted to be slightly coarser in grain-size (very fine sand) and therefore these variations in carbon perhaps represent sediment pulses, bringing in larger amounts of organic and inorganic carbon. Organic and inorganic carbon trends are similar, supporting the suggestion that the fluctuations in these values reflect variations in the carbon content of the basal debris layer of the glacier.

The LOI record suggests an ice front oscillation (Features 1 and 2; Figure 4.3). Organic and inorganic carbon declines from a peak at the base of the unit (Feature 1) up to the ice-wedge cast. The lag in the peak from the base of the section may be due to dilution of the organics by rapid coarser-grained sedimentation. Organic and inorganic carbon increases above the ice-wedge (Feature 2) followed by a slow decline to background values at about 120 cm. The ice-wedge

may record a retreat of the ice front. Retreat and readvance would allow for local vegetation recolonisation and the subsequent reintroduction of organic material to the basal zone of the glacier. The subsequent decline in organic and inorganic carbon would represent a return to normal subglacial sedimentation with its characteristic low carbon content.

Paleomagnetism

Two sets of samples were taken for paleomagnetic analyses from the east and west walls of the excavation. Set PE-W, collected in 2001, consists of cylinders and a 1 m u-shaped channel collected from the north face, which spanned all of Unit *I*-2. Set PE-E consists of cylinders collected in 2002 from the upper most 55 cm of Unit *I*-2 on the east wall of the excavation.

Paleomagnetic properties

Natural remnant magnetisation (NRM) is the natural magnetic moment per unit volume of rocks and sediments, and is dependent upon the mode of magnetic acquisition and the mineralogy of the media, as well as the concentration and grain size of the magnetic material. The source of the NRM in Port Eliza cave sediments is likely detrital magnetite. Minerals separated using a magnet and analysed by SEM-EDS display an iron peak, without titanium, suggesting that these grains are magnetite (Fe_3O_4) rather than other minerals such as ilmenite (FeTiO3). The magnetite peak may have been masked in XRD analysis due to its low proportions with respect to other minerals. Unit *I*-2 sediments display extremely high, strongly aligned NRM, indicating that most the magnetite grains were orientated in the same direction. This strong alignment likely reflects the very low energy of the depositional environment.

Three samples are described here; most samples show similar characteristics. BCW-008 (Figure 4.4) was analysed using a high number of demagnetisation steps and was used, along with several other samples, to determine the optimum number of demagnetisation steps for analysis of

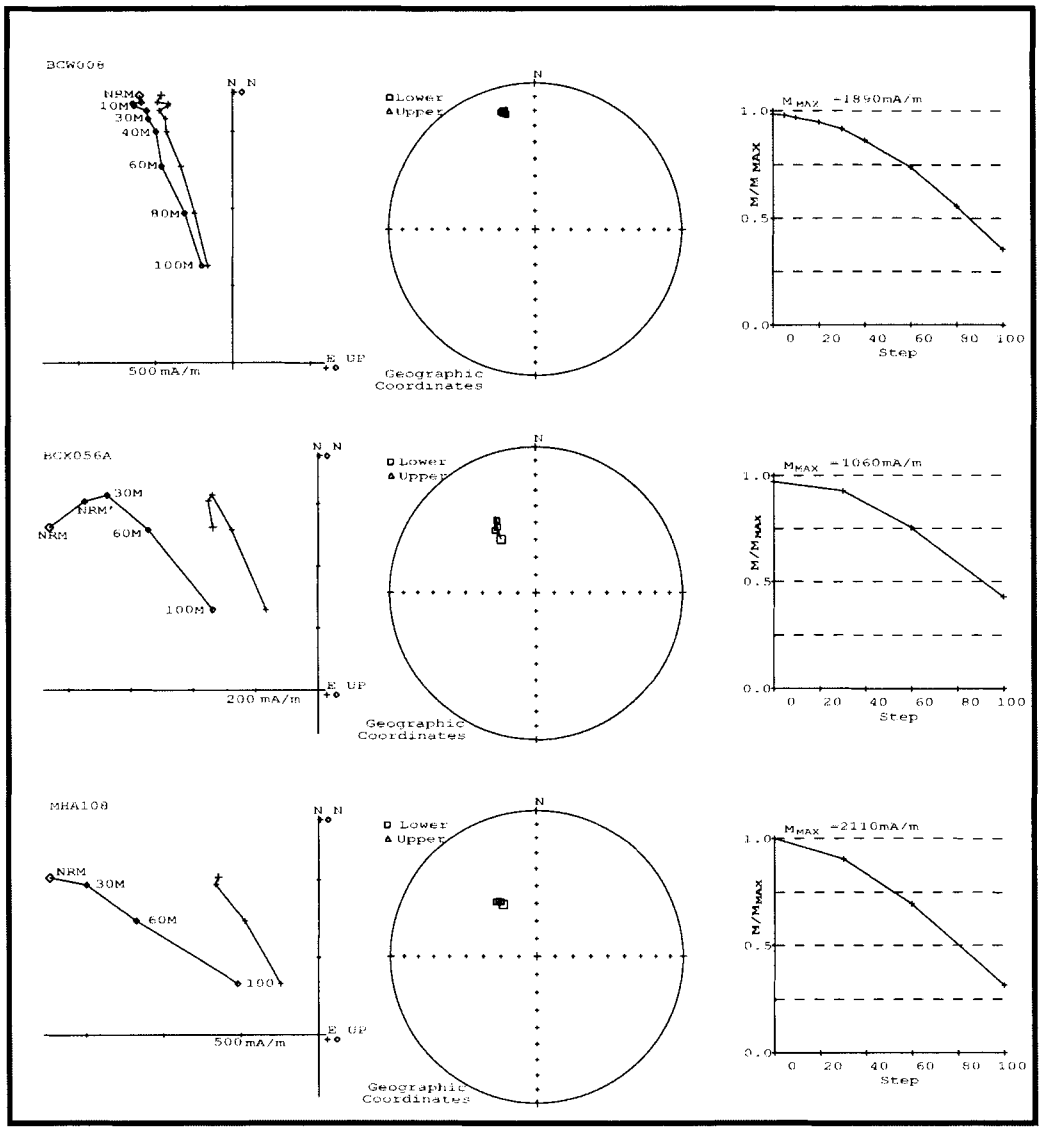

Figure 4.4. Demagnetisation plots of representative samples from Unit *I*-2.

other samples. BCX-056A (Figure 4.4) shows a small overprint, and MHA-108 (Figure 4.3) is typical of samples collected during the 2001 and 2002 field seasons.

The anisotropy of magnetic susceptibility (AMS) is a measure of the degree of consistency of magnetic grain orientations. Unit *I*-2 has extremely high anisotropy, indicating that the NRM is significantly shallower than the paleofield. Anisotropy values are up to 15%, much higher than those in typical samples of sedimentary rock (<3%). Data from these samples also indicate a horizontal foliation, with a vertical minimum axis. The foliation indicates compaction of the grains into the surface plane of the sediment, and is most evident in the lower part of the section, below 200 cm.

Koenigsberger ratios are a measure of the efficiency at which a sample has been magnetised. When the Koenigsberger ratios are high, each grain is contributing to the magnetisation, conversely when the ratios are low there is little alignment of the grains. In the sediments of Port Eliza cave the Koenigsberger ratios are commonly greater than 10 and some exceed >100 (values range from 1.7 to 122.5). These values are up to 1000 times greater than those of typical sediments and are comparable to values of sediments that have been struck by lightening, some lavas, and deposits of diagenetic, magnetic minerals or Chemical Remnant Magnetisation (CRM). Typical sedimentary rocks have Koenigsberger ratios of 0.05 to 0.5. In comparison, the average value in Unit *I*-2 is 54 with typical examples such as BCX-056A measuring 68.2 and high values such as 120.5 seen in sample BCW-008, not uncommon.

The most likely reason for the very high NRM and Koenigsberger ratio values is the calm conditions under which Unit *I*-2 was deposited. Further more, the sediments were derived largely from magnetite-bearing volcanic rocks. Under the calm conditions existing in the cave, minerals settled slowly from suspension, facilitating strong alignment with the geomagnetic field at the time of deposition. The horizontal foliation recorded in the AMS implies that the grains settled

with their long axis parallel to the bedding plane, and thus the magnetic axes were not as steep as the ambient field at the time.

Another possible explanation for the high NRM and Koenigsberger values is authigenic growth of magnetic minerals, some of which were noted in thin section. The highest Koenigsberger values correspond roughly to levels at which authigenic crystals of magnetite were seen in thin section. Precipitated crystals of magnetite would behave in a super-paramagnetic manner; i.e. below a certain grain size (typically < 0.03 μm) the grains behave, in a low field, like paramagnets and carry no remnance. This continues until the grain reaches a slightly larger size (its blocking volume, typically 0.1 μm in diameter), then they begin to carry a strong stable remnance. Therefore, if the authigenic crystals grow above their blocking volume, they can acquire the magnetic field at the time of precipitation. This can be problematic, as it is very difficult to determine the time of precipitation. Consequently, CRM can be acquired well after deposition, introducing a source of error to the data set. This scenario is, however, unlikely as authigenic growths are rare in thin section and most large magnetite grains were determined to be detrital.

Record of secular variation

The PE-W declination and inclination record displays smooth swings characteristic of hundreds to a few thousand years of geomagnetic secular variation (Figure 4.5). From the base, declination swings sharply from - 50° to + 20° between 280 and 270 cm depth. Declination then slowly decreases to 0° at 210 cm. There are minor variations in declination between 210 and 110 cm, but inclination, swings from 25° at 200 cm to 50° at 210 cm and remains high to just below 120 cm. There does not appear to be a major hiatus in the record in the vicinity of the ice-wedge cast, although inclination increases there. At about 100 cm, declination swings to 50° west of

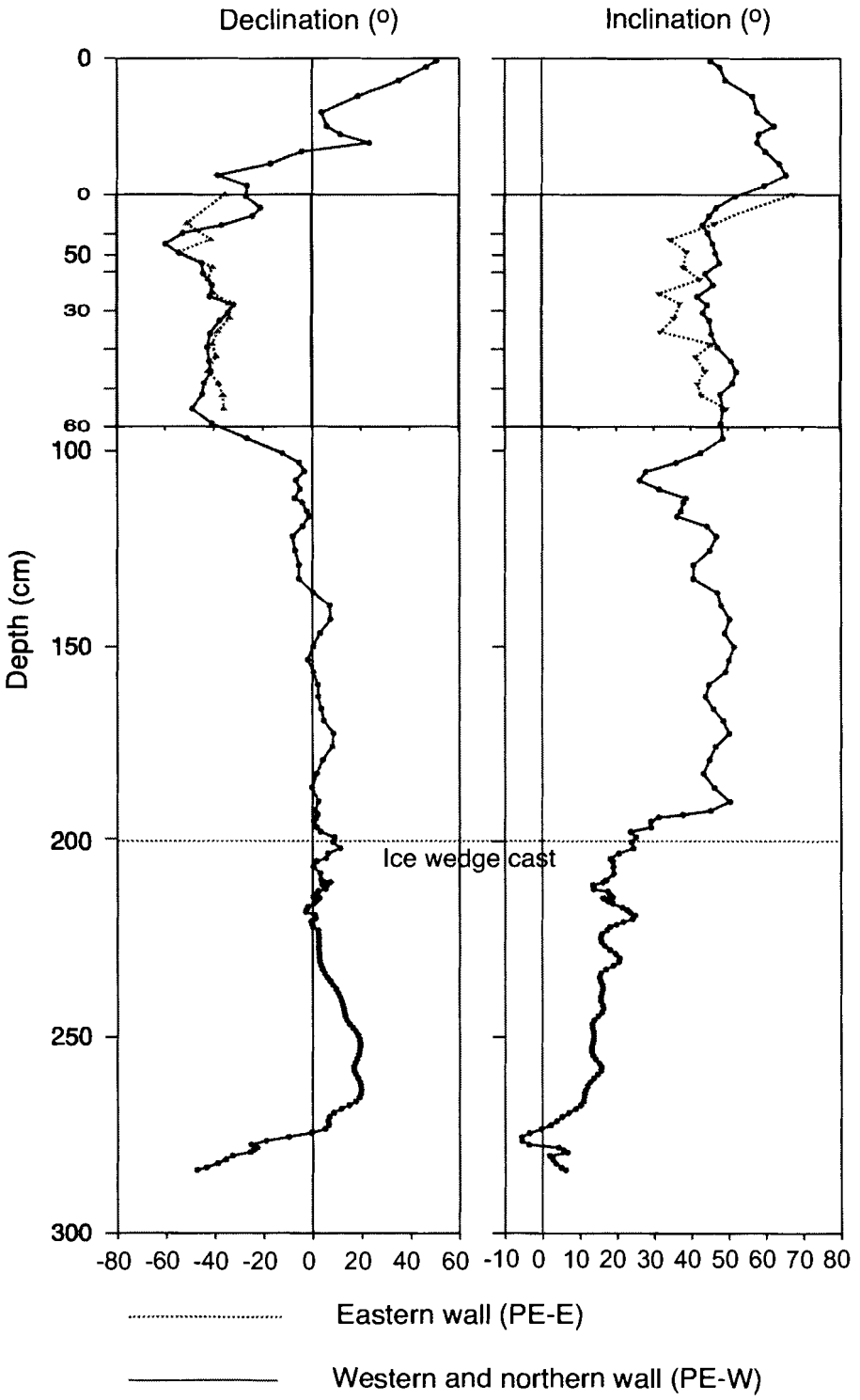

Figure 4.5. Declination and inclination of sediments in Unit I-2.

north associated with an increase in inclination from 30° up to 50°. At 50 cm, declination swings back east with a corresponding decrease in inclination.

PE-E is a much shorter record, taken from the east wall of the excavation (Figure 4.5). Declination averages, roughly 40° west of north, but reaches a maximum of 60° west of north at a depth of 3 cm. Inclination is approximately 40°, but increases to 70° at the top of the record. The PE-E record correlates well both in declination and inclination to the upper part of PE-W (Figure 4.5). Some offset between the two sides of the excavation is indicated by matching the two records. The eastern side (PE-E) is offset about 30 cm with respect to the western wall (PE-W) (Figure 4.5). The faulting has not altered the orientation of the sediments; the record of secular variation preserves the ambient field at the time of deposition.

An attempt was made to correlate the secular variation within the Port Eliza cave sediments with other records to better relate the sequence. However, there are few records spanning the LGM in North America. The nearest well dated record available is from Mono Lake, California (MLC) (Lund *et al.*, 1988) more than 1500 km south of Port Eliza.

Bounding ages for Unit *I*-2, to guide correlation, were derived from maximum and minimum radiocarbon ages (Figure 4.1) and other studies that indicate deglaciation *ca.* 13 ka BP (e.g., Blaise *et al.,* 1990; Howes, 1997; Nagorsen and Keddie, 2000). The longer PE-W record was filtered using a five-point running average. The most notable feature for correlation is an upward swing in declination from, east of north to west of north (D23 to D22, Figure 4.6) in the MLC record, with the maximum westward declination dated to *ca.* 14.8 ka BP (Lund *et al.,* 1988; S. Lund, personal communication, 2004). This swing was correlated with a similar trend in the Port Eliza record, and provided a datum to which the rest of the curve could be related. The other prominent feature that tied the two records together is the double peak in declination, in D23 in the Mono Lake record, which is present in the lower portion of the Port Eliza record. Correlation

was made by comparing overall trends or swings, rather than attempting to match each point of the records and was largely based on variations in declination above variations in inclination. The declination was chosen for primary correlation because of the high anisotropy values, which would have a major affect on the inclination of the Port Eliza record. Once the overall trends were correlated, the Port Eliza record was clipped and stretched to match the scale of the Mono Lake record. This helps to better visualise the correlation and the variation in sedimentation rates.

Two correlations are presented here as possible estimates for the duration of ice cover at Port Eliza (A and B; Figures 4.6, 4.7). The prominent swing of D23 to D22 noted in the Port Eliza cave record dates to *ca.* 14.8 ka BP (Lund *et al.,* 1988; Lund, personal communication, 2004) and provides the best estimate of the age of the sediments in the middle of Unit *I*-2. In both correlations the lower part of the record is fairly well constrained. The ice-wedge cast, in both these records, is estimated to be very close in age *ca.*15.9 ka BP in A and *ca.* 15.8 ka BP in B. The two correlations presented offer different estimates of the onset of ice cover. The Port Eliza declination curve swings west of 0° at its base, correlating with a swing in the MLC curve. In correlation A the onset of glaciation is estimated at *ca.* 16.2 ka BP, while in correlation B the onset is closer to 16 ka BP. Correlation A is more consistent with the radiocarbon age on the sparrow bone from Unit *I*-1 at 16, 270 $\pm$ 170 BP.

The estimates of deglaciation also differ between the two correlations. The top of the Port Eliza record swings west of 0° and can be correlated to either of two westward swings in the Mono Lake record. Correlation A estimates the timing of this swing to be close to *ca.* 13 ka BP. This is consistent with other studies that indicate deglaciation on Vancouver Island by 13 ka BP (e.g., Blaise *et al.,* 1990; Howes, 1997; Nagorsen and Keddie, 2000). Correlation B has deglaciation earlier ca. 13.4 ka BP.

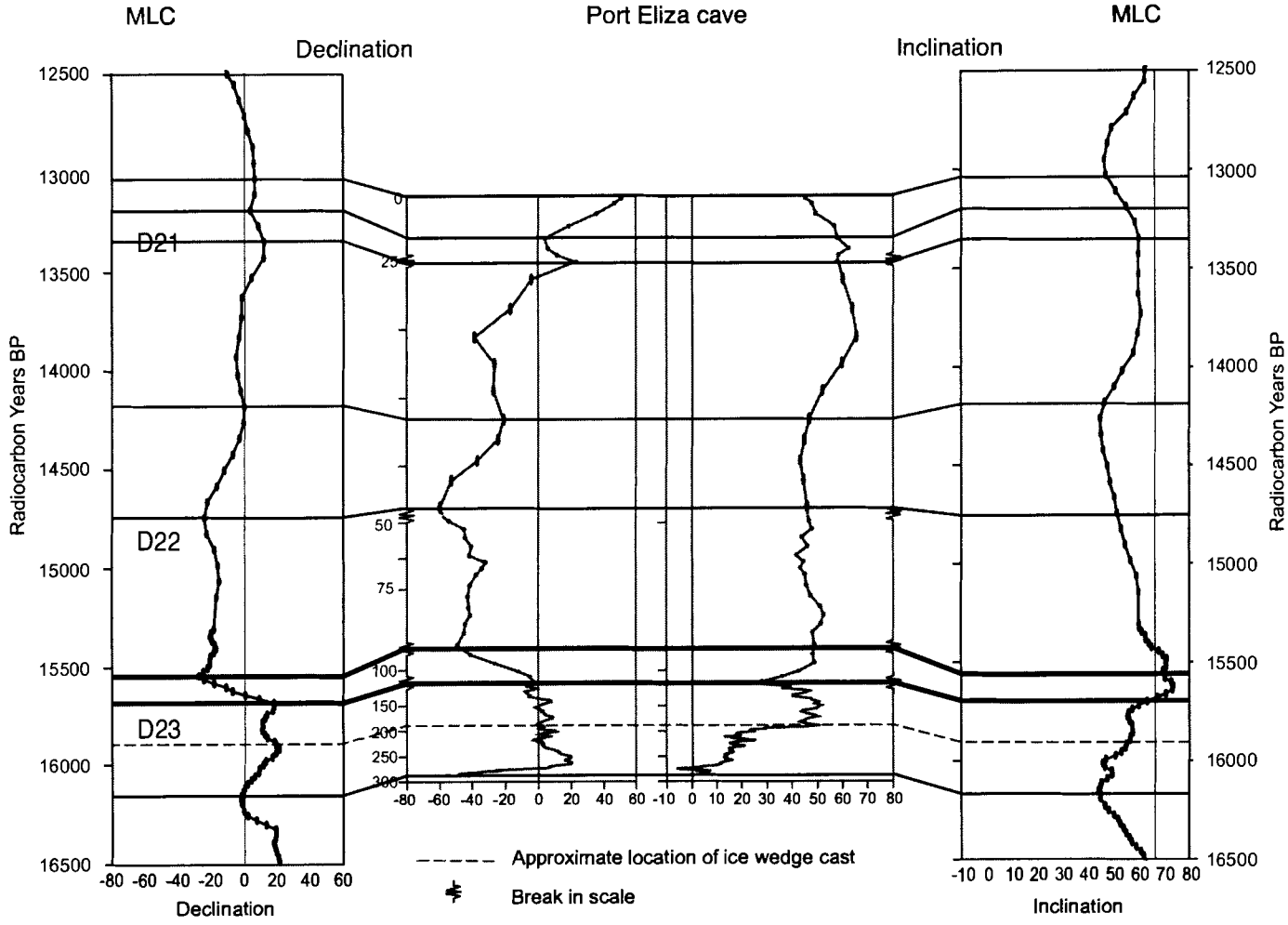

Figure 4.6. Correlation A. Port Eliza cave sediment paleosecular variation curve correlated with that of the Mono Lake record (MLC). Note the breaks in scale for the Port Eliza record utilised to improve correlation. Bold lines indicate more robust correlation points.

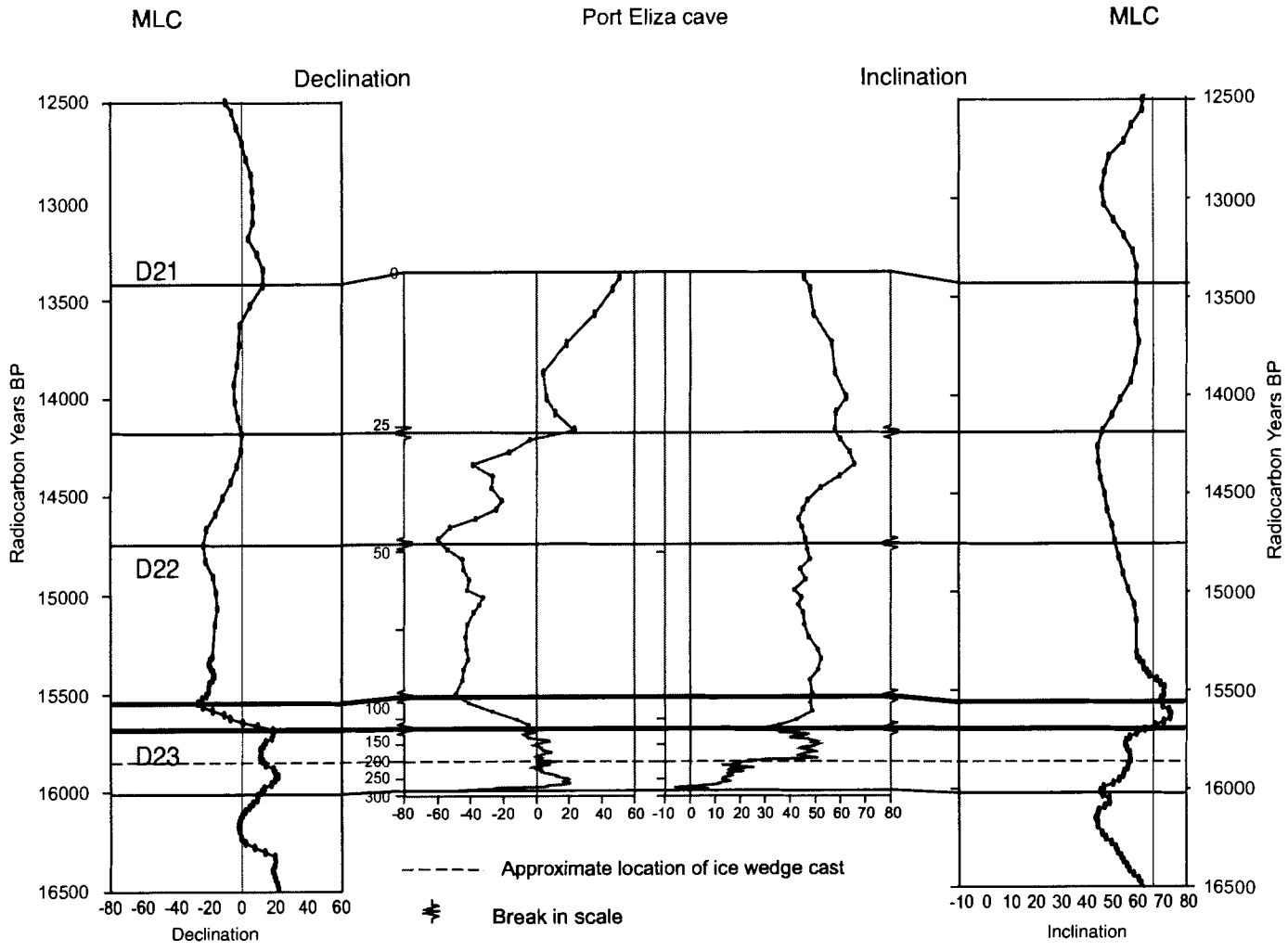

Figure 4.7. Correaltion B. Port Eliza cave sediment paleoscular variation curve with that of the Mono Lake record (MLC).

See previous.

The two correlations to the MLC also indicate variable sedimentation rates. In correlation A, *ca.* 15.5 ka BP, sedimentation rates were up to approximately 3.1 mm/yr. Between *ca.* 15.5 ka BP and *ca.* 13.3 ka BP sedimentation slowed to approximately 0.25 mm/yr, and then increased to approximately 0.83 mm/yr up to deglaciation at *ca.* 13 ka BP. Such variation is not unexpected because there is likely to be more sediment entering the cave soon after initial ice cover, which would decline as the glaciation reached it's maximum. The increase towards the end of the record could reflect increased melting associated with retreat of the ice. In correlation B there is progressively slower sedimentation throughout the sequence: 4.4 mm/yr between *ca.* 16 ka BP and *ca.* 15.5 ka BP; 0.73 mm/yr between *ca.* 15.5 ka BP and ca. 14, 750 BP; and down to 0.19 mm/yr before deglaciation at *ca.* 13.4 ka BP.

Of the two correlations the A correlation is favoured here for four reasons. The first is that although the primary correlation was made to the declination, the inclination in the first correlation matches well with the inclination record of Mono Lake. Secondly; the onset of glaciation at the base of the record is not clear; however, the difference between the first correlation and the second is only on the order of 200 years and the first estimate is more consistent with the youngest age from Unit *I*-1 on sparrow of 16, 270 $\pm$ 170. The third reason is that the date of deglaciation is consistent with other estimates of deglaciation for Vancouver Island (e.g., Blaise *et al.,* 1990; Howes, 1997; Nagorsen and Keddie, 2000). Finally the variations in sedimentation indicated by the first correlation are more consistent with sedimentary observations in Unit *I*-2, and those that would be expected over the course of a glaciation (i.e. rapid early deposition, followed by slow deposition at the peak of the glaciation and a return to more rapid deposition due to increased melting as deglaciation commenced).

Several potential sources of error exist in both the correlations and dating. One source of error is the possibility of hiatuses in the record. There is only one obvious break, represented by

the two ice-wedge casts, which occur at the same horizon, and the paleomagnetic record indicates that this hiatus was likely short. No other obvious breaks in sedimentation are evident in the sedimentary record although some could be present. Authigenic magnetite precipitates were noted in thin section, suggesting that chemical remnant magnetisation could influence the paleomagnetic record. They only occur sporadically, however, and are thought to have a limited effect on the paleomagnetic record. Another source of error is spatial differences in the Earth's geomagnetic field. Lund (1996) showed that there is variation in the paleomagnetic record between sites in North America. Another problem is potential errors in ages at sites (Verosub *et al.,* 1986). Variations in sedimentation rates at Mono Lake may also contribute error (Lund *et al.,* 1988; S. Lund, personal communication, 2004). It is difficult to estimate the uncertainty in the ages derived for the onset of ice cover and the ice-wedge feature, but it is likely several hundred years; studies of ice-wedge growth on Ellesmere Island determined low end rates of lateral growth to be 2-5 mm/yr (Lewkowicz, 1994). The large ice wedge cast at Port Eliza cave measured 110 cm, and assuming growth rates of 2-5 mm/yr, indicates a maximum of 220 to 550 years of growth. The assumed growth rates depend on similar sediment types and environmental conditions on Ellesmere Island today, and in Port Eliza cave *ca.* 15.7 ka BP. Based on sedimentological, observations and paleomagnetic analysis I favour a short growth period, for the ice-wedge, of 200 years or less.

Discussion

Synchronicity of climatic change across the Northern Hemisphere has long been a topic of discussion. The peak of the Vashon Stade in the Pacific Northwest has been correlated with Heinrich Event One (H1), and the Port Moody Interstade with Interstade Two of the Dansgaard-Oechger cycles (Hicock *et al.*, 1999, Lian *et al.,* 2001). Benson *et al.* (1998) show that, in the Mono Lake record, lake level fluctuations correlate with Dansgaard-Oechegar, Heinrich and

Milankovitch cycles. The record at Port Eliza cave is short (<3000 years), but spans the onset of local ice cover and the peak of the Fraser Glaciation. In the Port Eliza record, the peak of the Fraser Glaciation is thought to be represented by the decline in organic and inorganic carbon just above LOI feature 2 (Figure 4.6). This feature occurs above the ice-wedge cast and can be correlated through the paleosecular variation record to feature D22 (14.8 ka BP) in the MLC. This is consistent with the maximum of the Puget Lobe which is dated to 14, 890 $\pm$ 70 BP (Porter and Swanson, 1998). The timing of feature 2 also supports the suggestion of Hicock *et al.* (1999) and Lian *et al.* (2001) that the peak of the Fraser Glaciation is contemporaneous with H1 (*ca.* 14.8 ka BP), and also strengthens arguments for a coupling of North Atlantic and northeastern Pacific climatic oscillations.

The ice-wedge cast signals some climatic or glaciologic event. Two scenarios may have lead to the formation of this feature. The first scenario involves a change in subglacial hydrology. Water drains from the cave, allowing the sediment to freeze and the ice-wedge cast to form. The second scenario involves retreat of the ice front, which also would cause water to drain from the cave, and the ice-wedge to form. The second scenario is preferred for two reasons. First, if the cave remained closed by ice, isothermal conditions would have persisted, making it difficult to generate the necessary freezing and thawing cycles that form the ice-wedge casts. Second, organic carbon increases above the ice-wedge cast (Feature 2; Figure 4.3), as it did when the cave was first covered by ice. Retreat of the ice would allow for a localised plant recolonisation and provide organic material which would be incorporated in the ice during the re-advance. This best explains the prominent peak in organic carbon after the formation of the ice wedge. The ice-wedge cast formed approximately 500 years after ice initially covered the cave, a time when a localised fluctuation of the ice front is likely. No evidence exists for a fluctuation of the Puget Lobe *ca.* 15.7 ka BP (Porter and Swanson, 1998) or for a re-advance on Vancouver Island.

Because the secular variation curve implies only a short break in sedimentation associated with the ice-wedge, a local (i.e. non-regional climate-driven) oscillation of the ice front is assumed.

The sediments of Unit *I*-2 also provide information on subglacial conditions in the area at the maximum of the Fraser Glaciation. The short break in sedimentation at the time of ice-wedge formation is the only identified hiatus in sedimentation and indicates that these sediments represent nearly continuous deposition. Paleomagnetic data from raised sea caves in Norway display periods of non-deposition thought to represent periods of cold-based ice when the cave waters froze (Valen *et al.*, 1996). Thus the continuous sedimentation at Port Eliza cave indicates that the Cordilleran Ice Sheet, on the outer coast of Vancouver Island, was likely warm-based throughout the LGM.

Conclusion

The sediments of Unit *I*-2 in Port Eliza cave provide a record of paleosecular variation between *ca.* 16 and 13 ka BP and elucidate the character and timing of glaciation on the west coast of Vancouver Island. The paleomagnetic properties, grain size, and structure of the sediments, indicate deposition in a very low energy environment. Rhythmites in the upper portion of the sequence have characteristics of varves, but it is not possible to confirm annual sedimentation or how much of the sequence might be varves. The paleomagnetic record is characterised by smooth swings in declination and inclination, indicating a largely continuous record of deposition over hundreds or thousands of years. It is the first record of secular variation from this time period in British Columbia and could prove useful in future cave research.

Approximate ages were assigned to features in Unit *I*-2. Based on correlation of the Port Eliza paleosecular variation curve with that from Mono Lake the onset of ice cover likely occur about 16.2 ka BP. A short-lived hiatus in sedimentation associated with formation of an ice-

wedge cast occurred *ca.* 15.7 ka BP and is thought to represent a short-lived retreat of the ice front. The record of largely continuous sedimentation suggests that warm-based ice existed in this area at the LGM. The ages for this unit, derived from both maximum and minimum radiocarbon ages and paleomagnetic correlation are consistent with the general global pattern of glaciation during the late Wisconsinan and indicate that the Vashon maximm coincided with Heinrich Event One, as it does in the Fraser Lowland.

This study has shown that the application of multiple methods of analysis to studies of cave sediments can be an effective tool in elucidating the character of glaciation. Future work on raised sea caves will resolve the timing of glaciation on the outer coast of B.C. and provide paleoclimatic and glaciologic information on the Cordilleran Ice Sheet. Caves with a longer stratigraphic record than Port Eliza cave may provide superior resolution of older glaciations, which currently remain poorly understood.

CHAPTER FIVE

DISCUSSION, CONCLUSION AND FUTURE WORK

Discussion

This thesis documents two, very different, late Wisconsinan environments at Port Eliza cave on the west coast of Vancouver Island. Chapter Three focuses on the period from about 18 to 16 ka BP, before the cave was glaciated. Chapter Four focuses on the period from about 16 to 14 ka BP. Here, I discuss these two periods in the context of the stratigraphy of Vancouver Island and of the Fraser Lowland, and discuss the regional and global significance of the results.

Glaciers advanced into the Fraser Lowland *ca.* 21.5 ka BP during the Coquitlam Stade, (Hicock and Armstrong, 1981). This advance was followed by retreat during the Port Moody Interstade *ca.* 18.7 ka to 17.6 ka BP (Lian *et al.*, 2001). The subsequent Vashon Stade represents full-glacial conditions and the peak of the Fraser Glaciation. In contrast, only one advance is recorded on Vancouver Island during the Fraser Glaciation. Quadra Sand, which records an ice advance in the Strait of Georgia, is capped by a single (Vashon) till (Clague, 1981). Howes (1981, 1983) refers to a similar, although diachronous event on northern and central Vancouver Island. Gold River Drift, on central Vancouver Island, indicates that glaciation started early and well-advanced by *ca.* 25 ka BP (Howes, 1980). Parts of northern Vancouver Island became ice-covered before 20 ka BP (Howes, 1983). The sediments of Port Eliza cave indicate that the west coast was not glaciated until *ca.* 16 ka BP much later than other areas of Vancouver Island (Ward *et al.*, 2003).

It is difficult to be certain that Vancouver Island did not experience a double advance similar to that documented in the Fraser Lowland. Evidence of the Port Moody Interstade on Vancouver Island may have been removed by advancing ice. At Port Eliza cave, ages derived for Unit *I*-1 overlap that of the Port Moody Interstade (Figure 5.1); however, without further exposure of the section, it is not possible to establish whether it represents a period of ice retreat, like the Port Moody Interstade, or simply indicates that ice had not yet reached the coast. Paleoenvironmental evidence suggests significant differences between the two areas.

In the Fraser Lowland, Port Moody Interstade sediments indicate a temperate moist climate and an open spruce-fir forest (Lian *et al.*, 2001). The sediments of Unit *I*-1, in contrast, suggest a cold climate with rare trees. The difference could be due to a steep climatic gradient between the two sites. More likely, however, is that the pollen from Unit *I*-1 is younger than the Port Moody Interstade sediments in the Fraser Lowland and records cooling just before the LGM.

A one-advance scenario is favoured here. The stratigraphic evidence at Gold River and Port McNeill (Howes, 1981, 1983) supports this scenario. The advance and retreat inferred from Unit *I*-2 occured early in the Vashon Stade and were of short duration, probably localised events before full-glacial conditions were established.

These results are significant, not only regionally, but also in terms of the wider debates surrounding human migration to North America and the synchronicity of global climate change. The sediments of Unit *I*-1 provide insight into the character of the environment on the west coast of Vancouver Island just before the LGM and its ability to sustain humans. Ungulate bones and other fossil fauna indicate the presence of large animals and abundant marine food resources. The duration of glaciation is also significant to this debate, with ice cover being relatively short-lived on the outer coast of Vancouver Island. The correlation between the Vashon Stade and Heinrich

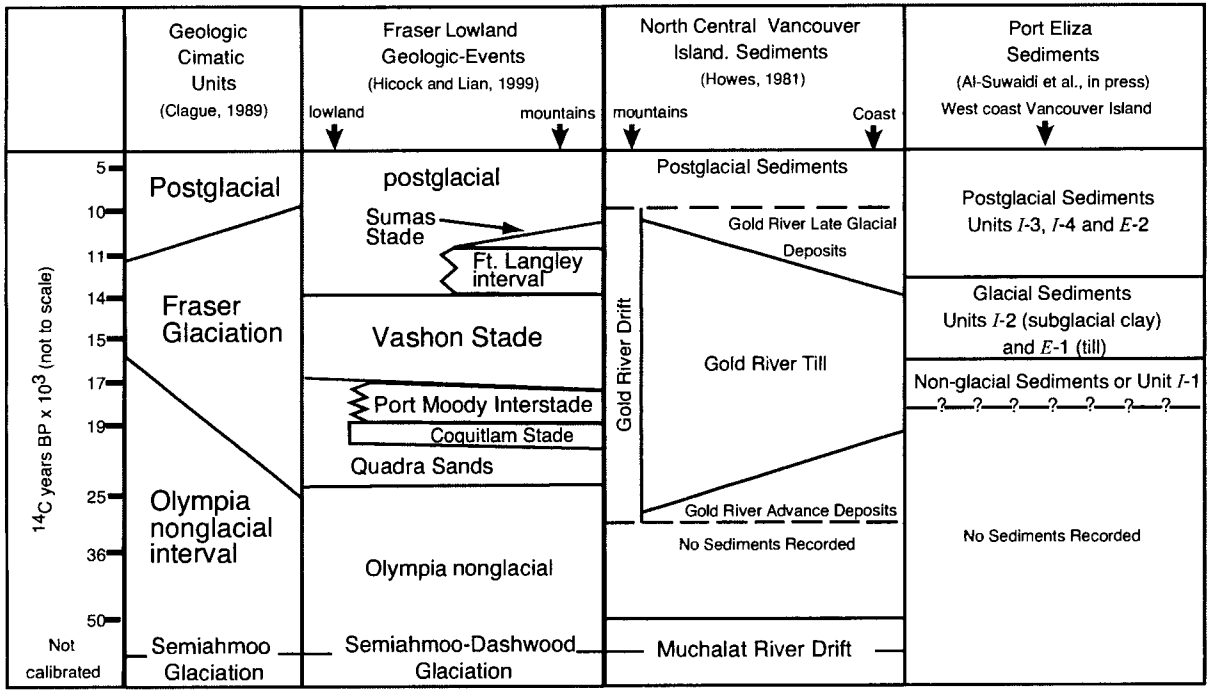

Figure 5.1. Relation between sediments of Port Eliza cave and geologic-climatic units of British Columbia, geologic events of the Fraser Lowland, and the sediments of north-central Vancouver Island.

Event One was first suggested by Lian *et al.* (2001). This correlation is supported by the record from Port Eliza cave.

Conclusion

Sediments of coastal wave-cut caves can be used effectively to reconstruct Pleistocene environments in Canada. Using multiple methods, I have improved understanding of nonglacial, glacial and deglacial environments on the west coast of Vancouver Island during the late Wisconsinan Fraser Glaciation. Plant macro-fossil, pollen, and faunal data indicate a cold, dry, steppe environment with rare trees and a diverse faunal assemblage just before the LGM. Radiocarbon and U/Th dating supported by paleomagnetic data constrain the age of sediments and, more importantly, ice cover at Port Eliza cave to between *ca.* 16 ka and 13 ka BP. LOI, sedimentologic, and paleomagnetic data show that there was continuous sedimentation during this period and imply that the Cordilleran Ice Sheet in this area was dominantly warm-based. A short-lived retreat and readvance, *ca.* 15.7 ka BP, is inferred from an ice-wedge cast in Unit *I*-2. Age constraints on glacial sediments in Port Eliza cave indicate that maximum late Wisconsinan glaciation on the west coast of Vancouver Island coincide with Heinrich Event One.

The near-continuous record of subglacial sedimentation at Port Eliza cave permits detailed interpretation of the timing and character of the LGM. The sediments are contemporaneous with the Vashon Stade (Figure 5.1). A maximum age of glaciation of 16.2 ka BP, based on sparrow bone, is corroborated by paleomagnetic correlation with the Mono Lake paleomagnetic record. The paleomagnetic record also shows that an ice-wedge formed *ca.* 15. 7 ka BP. It suggests that sedimentation rates were higher prior to formation of the ice-wedge than afterward, as the peak of the LGM was reached. LOI analysis indicates an oscillation during glacier advance. An early advance that covered the cave was followed by retreat, during which the ice-wedge cast formed. Organic and inorganic carbon declined toward the peak of the LGM.

Given that support for the inland "Ice Free Corridor" has declined (Jackson *et al.*, 1996), more focus should now be placed on the coastal migration hypothesis of Fladmark (1979). This research has shown, not only that there was a window of opportunity for early human migration along the coast, but also that the environment could have sustained human populations. This thesis has shown that cave deposits can provide a wealth of information in the study of paleoenvironments. Future work in raised sea caves has a high potential to provide longer records of late Pleistocene paleoenvironments, paleoecology and paleomagnetism.

Recommendations for future work

Future work should concentrate on the discovery of more caves, with which to compare the results of Port Eliza cave. The most promising aspect of this research is the possibility of longer sediment records, than that of Port Eliza cave, being present. There is currently a lack of sites which preserve pre-late Wisconsinan sediments, due to glacial erosion. Raised sea caves have a high potential for preserving glacial and non glacial sediments and therefore warrant further investigation. Here are several other areas of this research which bear further investigation:

1. Further study of the laminated sediments is required to establish whether these sediments represent annual or sub-annual varves. This would be very useful in particular for developing the paleomagnetic record of these sediments, the strength of which is hindered by a lack of control on sedimentation rates.

2. More detailed X-Ray diffraction analysis of the clay sediments may be useful in establishing provenance. It may also address the reasons for high NRM but a lack of magnetite peaks in XRD analysis.

3. A few of the samples analysed by XRD displayed a significant calcite peak which was not seen in most samples. Several explanations were put forward for this including: changes in glacier sediment source, changes in source waters (ground water vs glacial water) or, the favoured explanation, that the calcite may indicate short term open cave (i.e. water free) conditions, under which calcium carbonate could be precipitated. A simple test using dilute HCl could be carried out, at high resolution (down to individual laminae). This test could provide a proxy for open cave conditions as well as answering questions of whether its recurrence is sub-annual, annual or at larger time scales.

4. Isotope studies of speloethem deposits from raised-sea caves or karst caves may yield high resolution paleoenvironment data for the late Wisconisnan period. Following from the early work of Gascoyne *et al.* (1981) and given the success of related research in other regions, isotope research of speloethem deposits needs to be developed in western Canada.

REFERENCE LIST

Adovasio, J. M. and Pedler, D. R. 1997. Monte Verde and the antiquity of human kind in the Americas. Antiquity. **71:** 573-580.

Al-Suwaidi, M., Ward, B. C., Wilson, M. C., Hebda, R. J., Nagorsen, D. W., Marshall, D., Ghaleb, B., Wigen, R. J. and Enkin, R. J. In Press. Late Wisconsinan Port Eliza cave Deposits and their implications for human coastal migraiotn, Vancouver Island, Canada. Geoachaeology.

Allen, G. B., Brown, K. J. and Hebda, R. J. 1999. Surface pollen spectra from south Vancouver Island, British Columbia, Canada. Canadian Journal of Botany. **77:** 786-789.

Allen, J. and Holloway, J. S. 1995. The continuity of Pleistocene radiocarbon determinations in Australia. Antiquity. **69:** 101-112.

Armstrong, J. E. 1981. Post-Vashon Wisconsin glaciation, Fraser Lowland, British Columbia. Geological Survey of Canada, Bulletin. **322:** 34.

Armstrong, J. E. and Clague, J. J. 1977. Two major Wisconsin stratigraphic units in southwest British Columbia. Canadian Journal of Earth Sciences.

Barrie, J. V. and Conway, K. W. 1999. Late Quaternary glaciation and post-glacial stratigraphy of the Northern Pacific Margin of Canada. Quaternary Research. **51:** 113-123.

Benson, L. V., Lund, S. P., Burdett, J. W., Kashgarian, M., Rose, T. P., Smoot, J. P. and Schwartz, M. 1998. Correlation of late-Pleistocene lake-level oscillations in Mono Lake, California, with North Atlantic climate events. Quaternary Research. **49:** 1-10.

Blaise, B., Clague, J. J. and Mathewes, R. W. 1990. Time of maximum late Wisconsinan Glaciation, west coast of Canada. Quaternary Research. **47:** 140-146.

Brauner, D. 1985. Early Human Occupation in the Uplands of the Southern Plateau: Archaeological Excavations at the Pilcher Creek Site, Union County, Oregon. Department of Anthropology, Oregon State University.

Brigham-Grette, J., Lozhkin, A. V., Anderson, P. M. and Glushkova, O. Y. 2004. Environmental conditions in Northeast Asia and Northeastern North America. *In* Entering America: Northeast Asia and Beringia before the Last Glacial Maximum. *Edited by* D.B. Madsen. The University of Utah Press, pp 29-61.

Bryant, A. A. and Janz, D. W. 1996. Distribution and abundance of Vancouver Island marmots (*Marmota vancouverensis*). Canadian Journal of Zoology. **74:** 667-667.

Bryan, A. L. and Tuohy, D. R. 1999. Prehistory of the Great Basin/Snake River Plain to about 8,500 years ago. *In* Ice Age Peoples of North America. *Edited by* R. A. Bonnichsen and K. L. Turnmire. Oregon State University Press, pp 249-263.

Cannon, A. 2000. Settlements and sea-levels on the central coast of British Columbia: evidence from shell midden cores. American Antiquity. **65:** 67-77.

Carlson, R. L. 1996a. Introduction to early human occupation in British Columbia. *In* Early Human Occupation in British Columbia. *Edited by* R. L. Carlson and L. D. Bona. UBC Press, pp 3-10.

Carlson, R. L. 1996b. Early Namu. *In* Early Human Occupation in British Columbia. *Edited by* R. L. Carlson and L. D. Bona. UBC Press, pp 83-102.

Cinq-Mars, J. 1979. Bluefish Cave I: A late Pleistocene eastern Beringian cave deposit in the northern Yukon. Canadian Journal of Archaeology. **3:** 1-32.

Cinq-Mars, J. and Morlan, R. E. 1999. Bluefish Caves and Old Crow Basin: A new report. *In* Ice Age People of North America. *Edited by* R. Bonnichsen and K. L. Turnmire. Oregon State University Press, pp 200-212.

Clague, J. J. 1981. Late Quaternary geology and geochronology of British Columbia; Part 2, Summary and discussion of radiocarbon-dated Quaternary history. Paper - Geological Survey of Canada.

Clague, J. J. 1989. Quaternary geology of the Canadian Cordillera. *In* Quaternary Geology of Canada and Greenland. *Edited by* R. J. Fulton. Geological Survey of Canada, Geology of Canada, no. 1, pp 17-83.

Clague, J. J., Armstrong, J. E. and Mathewes, W. H. 1980. Advance of the Late Wisconsin Cordilleran Ice Sheet in southern British Columbia since 22,000 yr B.P. Quaternary Research. **13:** 322-326.

Clague, J. J., Barendregt, R., Enkin, R. J. and Foit, F. R. J. 2003. Paleomagnetic and tephra evidence for tens of Missoula floods in southern Washington. Geology. **31:** 247-250.

Clague, J. J. and Bobrowsky, P. T. 1990. *Holocene sea level change and crustal defromation, southwestern British Columbia.* Current research; Part E, Cordillera and Pacific margin paper. 245-250.

Clague, J. J., Mathewes, R. W. and Ager, T. A. 2004. Environments of northwestern North America before the Last Glacial Maximum. *In* Entering America: Northeast Asia and Beringia before the Last Glacial Maximum. *Edited by* D. B. Madsen. The University of Utah Press, pp 63-94.

Clague, J. J., Mathewes, R. W., Guilbault, J. P., Hutchinson, I. and Ricketts, B. D. 1997. Pre-Younger Dryas resurgence of the southwestern margin of the Cordilleran Ice Sheet, British Columbia, Canada. Boreas. **26:** 261-268.

Clague, J. J. and James, T. S. 2002. History and isostatic effects of the last ice sheet in southern British Columbia. *In* Ice Sheets and Sea Level of the Last Glacial Maximum. *Edited by* P. U. Clark and A. C. Mix. Quaternary Science Reviews **21**, 71-87.

Davis, L. G., Punke, M. L., Hall, R. L., Fillmore, M. and Willis, S. C. 2004. Evidence for a Late Pleistocene occupation of the southern Northwest Coast. Journal of Field Archaeology. **29:** 1-10.

Davis, L. G. and Sisson, D. A. 1998. An early stemmed point cache from the lower Salmon River Canyon of west-central Idaho. Current Research in the Pleistocene. **15:** 13-13.

Dillehay, T. D. 1989. Monte Verde. Science. **245:** 1436.

Dillehay, T. D. 1997. Monte Verde: A Late Pleistocene Settlement in Chile: Palaeoenvironmental and site context. Smithsonian Institution Press.

Dillehay, T. D. and Collins, M. B. 1988. Early cultural evidence from Monte Verde in Chile. Nature. **332:** 150-152.

Dixon, E. J. 1999. Bones, Boats, & Bison: Archeology and the First Colonization of Western North America. University of New Mexico Press.

Duk-Rodkin, A. and Hughes, O. L. 1991. Age relationships of Laurentide and montane glaciations, Mackenzie Mountains, Northwest Territories. Geographie Physique et Quaternaire. **45:** 79-90.

Duk-Rodkin, A. and Hughes, O. L. 1992. Pleistocene montane glaciations in the Mackenzie Mountains, Northwest Territories. Geographie Physique et Quaternaire. **46:** 69-83.

Dyke, A.S. 2004. An outline of North American deglaciation with emphasis on central and northern Canada. *In* Quaternary Glaciations Extent and Chronology, Part II: North America *Edited by* J. Ehlers and P.L. Gibbard. Developments in Quaternary Science. Amsterdam Elsevier. **2**: 373-424

Edwards, R. L., Chen, J. H. and Wasserburg, J. G. 1987. ^{238}U-^{234}U-^{230}Th-^{232}Th systematics and precise measurement of time over the last 500,000 years. Earth and Planetary Science Letters. **81:** 175-192.

Faegri, K. and Iversen, J. 1989. Textbook of Pollen Analysis. Wiley.

Fedje, D. W. and Josenhans, H. W. 2000. Drowned forest and archaeology on the continental shelf of British Columbia, Canada. Geology. **28:** 99-102.

Fedje, D. W., Mackie, Q., Dixon, E. J. and Heaton, T. H. 2004. Late Wisconsinan environments and archaeological visibility on the Northern Northwest Coast. *In* Entering America: Northeast Asia and Beringia before the Last Glacial Maximum. *Edited by* D. B. Madsen. The University of Utah Press, pp 97-138.

Fedje, D. W., Wigen, R. J., Mackie, Q., Lake, C. and Sumpter, I. 2001. Preliminary results from investigations at Kilgii Gwaay: an early Holocene archaeological site on Ellen Island, Haida Gwaii, British Columbia. Canadian Journal of Archaeology. **25:** 98-120.

Fitzpatrick, E.A. 1984. Preparation of polished blocks and thin sections of soils. *In* Micromorphology of Soils. Chapman and Hall, London, U.K., pp. 6-50

Fitzpatrick, E.A. 1993. Soil microscopy and micromorphology. J. Willey, Chichester, New York.

Fladmark, K. R. 1979. Routes; alternate migration corridors for early man in North America. American Antiquity. **44:** 55-69.

Fladmark, K. R. 1983. Times and places: environmental correlates of mid- to late Wisconsinan human population expansion in North America. *In* Early Man in the New World. *Edited by* R. Shutler. Sage Publications, pp 13-41.

Gascoyne, M., Ford, D. C. and Schwarcz, H. P. 1981. Late Pleistocene chronology and paleoclimate of Vancouver Island determined from cave deposits. Canadian Journal of Earth Sciences. **18:** 1643-1652.

Gee, G. W. and Bauder, J. W. 1986. Particle-size analysis. *In* Methods of Soil Analysis, Part 1: Physical and Mineralogical Methods. *Edited by* A. Klute. Society of Agronomy/Soil Science Society of America.

Graham, R. W. and Graham, M. A. 1994. Late Quaternary distribution of Martes in North America. *In* Martens, Sables, and Fishers. Biology and Conservation. *Edited by* S. W. Buskirk, A. S. Harestad, M. G. Raphael and R. A. Powell. Comstock Publishing Associates/Cornell University Press, pp 26-58.

Grayson, D. K. 1984. Time of extinction and nature of adaptation of the noble marten, *Martes nobilis*. *In* Contributions in Quaternary Vertebrate Paleontology: A Volume in Memorial to John E. Guilday. *Edited by* H. H. Genoways and M. R. Dawson. Carnegie Museum of Natural History, Special Publication no. 8, pp 233-240.

Gustafson, C. E., Gilbow, D. and Daugherty, R. D. 1979. The Manis Mastodon site: early man on the Olympic Peninsula. Canadian Journal of Archaeology. **3:** 157-164.

Hamilton, T. D. and Goebel, T. 1999. Late Pleistocene peopling of Alaska. *In* Ice Age Peoples of North America: Environments, Origins, and Adaptations of the First Americans. *Edited by* R. A. Bonnichsen and K. L. Turnmire. Oregon State University Press, pp 156-199.

Heaton, T. H. and Grady, F. 2003. The Late Wisconsin vertebrate history of Prince of Wales Island, southeast Alaska. *In* Ice Age Cave Faunas of North America. *Edited by* B. W. Schubert, J. I. Mead and R. W. Graham. Indiana University Press, pp 17-53.

Heaton, T. H., Talbot, S. L. and Shields, G. F. 1996. An ice age refugium for large mammals in the Alexander Archipelago, southeastern Alaska. Quaternary Research. **46:** 186-192.

Hebda, R. J. 1983. Late glacial and post glacial vegetation history at Bear Cove Bog, northeast Vancouver Island, British Columbia. Canadian Journal of Botany. **61:** 3172-3192.

Hebda, R. J. and Allen, G. B. 1993. Modern pollen spectra from west central British Columbia. Canadian Journal of Botany. **71:** 1486-1495.

Hetherington, R., Barrie, J. V., Reid, R. G. B., Macleod, R. and Smith, D. J. 2004. Paleogeography, glacially induced crustal displacement, and late Quaternary coastlines on the continental shelf of British Columbia, Canada. Quaternary Science Reviews. **23:** 295-318.

Hetherington, R., Barrie, J. V., Reid, R. G. B., MacLeod, R., Smith, D. J., James, T. S. and Kung, R. 2003. Late pleistocene coastal paleogeography of the Queen Charlotte Islands, British Columbia, Canada, and its implications for the terrestrial biogeography and early post-glacial human occupation. Canadian Journal of Earth Sciences. **40:** 1755-1766.

Hicock, S. R. and Armstrong, J. E. 1981. Coquitlam Drift: a pre-Vashon Fraser glacial formation in the Fraser Lowland, British Columbia. Canadian Journal of Earth Sciences. **18:** 1443-1451.

Hicock, S. R., Hebda, R. J. and Armstrong, R. J. 1982. Lag of the Fraser glacial maximum in the Pacific Northwest: Pollen and macrofossil evidence from western Fraser Lowland, British Columbia. Canadian Journal of Earth Sciences. **19:** 2288-2296.

Hicock, S. R. and Lian, O. B. 1995. The Sisters Creek Formation: Pleistocene sediments representing a nonglacial interval in southwestern British Columbia at about 18 ka. Canadian Journal of Earth Sciences. **32:** 758-767.

Hicock, S. R. and Lian, O. B. 1999. Cordilleran Ice Sheet lobal interactions and glaciotectonic superposition through stadial maxima along a mountain front in southwestern British Columbia. Boreas. **28:** 531-542.

Hicock, S. R., Lian, O. B. and Mathewes, R. W. 1999. 'Bond cycles' recorded in terrestrial Peistocene sediments of southwestern British Columbia, Canada. Journal of Quaternary Science. **14:** 443-449.

Howes, D. E. 1981. Late Quaternary sediments and geomorphic history of north-central Vancouver Island. Canadian Journal of Earth Sciences. **18:** 1-12.

Howes, D. E. 1983. Late Quaternary sediments and geomorphic history of northern Vancouver Island, British Columbia. Canadian Journal of Earth Sciences. **201:** 57-65.

Howes, D. E. 1997. Quaternary geology of Brooks Peninsula. *In* Brooks Peninsula; An Ice Age Refugium on Vancouver Island. *Edited by* R. J. Hebda and J. C. Haggarty.

Ivanovich, M., Harmon, R.S., 1992. Uranium-series disequilibrium applications to Earth, Marine, and Environmental Sciences. Oxford Science publications, Clarendon press-Oxford.

Jackson, L. E. and Duk-Rodkin, A. 1996. Quaternary geology of the ice-free corridor: glacial controls on the peopling of the New World. *In* Prehistoric Mongoloid Dispersals. *Edited by* T. Akazawa and E. J. E. Szathmary. Oxford University Press, pp 215-227.

Jackson, L. E., Jr. and Wilson, M. C. 2004. The ice-free corridor revisited. Geotimes. **49:** 16-19.

Jackson, L. E. J., Phillips, F. M., Shimamura, K. and Little, E. C. 1997. Cosmogenic ^{36}Cl dating of the Foothills Erratics Train, Alberta, Canada. Geology. **25:** 195-198.

JCPDS 1993. Mineral Powder Diffraction File Data Book. JCPDS International Center for Diffraction Data.

Johnston, W. A. 1933. Quaternary geology of North America in relation to the migration of man. *In* The American Aborigines, Their Origin and Antiquity. *Edited by* D. Jenness. University of Toronto Press, pp 9-45.

Josenhans, H., Fedje, D. W., Pientz, R. and Southon, J. R. 1997. Early humans and rapidly changing Holocene sea levels in the Queen Charlotte Islands – Hecate Strait, British Columbia, Canada. Science. **277:** 71-74.

Karlen, W. 1981. Lacustrine sediment studies; a technique to obtain a continuous record of Holocene glacier variations. Geografiska Annaler. Series A: Physical Geography. **63:** 273-281.

Karlen, W. and Denton, G. H. 1976. Holocene glacial variations in Sarek National Park, northern Sweden. Boreas. **5:** 25-56.

Krinsley, D. H. and Doornkamp, J. C. 1973. Atlas of Quartz Sand Surface Textures. Cambridge University Press.

Larsen, E., Gulliksen, S., Lauritzen, S.-E., Lie, R., Lovlie, R. and Mangerud, J. 1987. Cave stratigraphy in western Norway; multiple Weichselian glaciations and interstadial vertebrate fauna. Boreas. **16:** 267-292.

Larsen, E. and Mangerud, J. 1989. Marine caves: on - off signals for glaciations. Quaternary International. **3/4:** 13-19.

Lewkowicz, A.G., 1994. Ice wedge rejuvination, Fosheim Peninsula, Ellesmere Island. Permafrost and Periglacial Processes, **5:** 251-268

Lian, O. B. and Hickin, E. J. 1993. Late Pleistocene stratigraphy and chronology of lower Seymour Valley, southwestern British Columbia. Canadian Journal of Earth Sciences. **30:** 841-850.

Lian, O. B., Mathewes, R. W. and Hicock, S. R. 2001. Paleoenvironmental reconstruction of the Port Moody Interstade, a nonglacial interval in southwestern British Columbia at about 18,000 ^{14}C years B.P. Canadian Journal of Earth Sciences. **38:** 943-952.

Lund, S. P. 1996. A comparison of Holocene paleomagnetic secular variation records from North America. Journal of Geophysical Research, B, Solid Earth and Planets. **101:** 8007-8027.

Lund, S. P., Liddicoat, J. C., Lajoie, K. R., Henyey, T. L. and Robinson, S. W. 1988. Paleomagnetic evidence for long-term (104 year) memory and periodic behavior in the Earth's core dynamo process. Geophysical Research Letters. **15:** 1101-1104.

Madsen, D. B. 2004. Colonization of the Americas before the Last Glacial Maximum: Issues and Problems. *In* Entering America: Northeast Asia and Beringia before the Last Glacial Maximum. *Edited by* D. B. Madsen. The University of Utah Press, pp 1-26.

Mandryk, C. A. S., Josenhans, H., Fedje, D. W. and Mathewes, R. W. 2001. Late Quaternary paleoenvironments of Northwestern North America: implications for inland versus coastal migration routes. Quaternary Science Reviews. **20:** 301-314

Mangerud, J., Reidar, L., Gulliksen, S., Hufthammer, A. K., Larsen, E. and Valen, V. 2003. Paleomagnetic correlations between Scandinavian Ice-sheet fluctuations and Greenland Dansgaard-Oeschger events, 45000-25000 yr. BP. Quaternary Research. **59:** 213-222.

Mann, D. H. and Peteet, D. M. 1994. Extent and timing of the late glacial maximum in Southwestern Alaska. Quaternary Research. **42:** 136-148.

Mathewes, R. W. 1989. Paleobotany of the Queen Charlotte Islands. *In* The Outer Shores. *Edited by* G. G. E. Scudder and N. Gessler. University of British Columbia, pp 75-90.

Mehringer, P. J., Jr. and F. Foit, J. 1990. Volcanic ash dating of the Clovis cache at East Wenatchee, Washington. National Geographic Research. **6:** 495-503.

Meltzer, D. J. 1997. Monte Verde and the Pleistocene peopling of the Americas. Science. **276:** 754-755.

Meltzer, D. J., Grayson, D. K., Ardila, G., Barker, A. W., Dincauze, D. F., Haynes, C. V., Mena, F., Nunez, L. and Stanford, D. J. 1997. On the Pleistocene antiquity of Monte Verde, Southern Chile. American Antiquity. **64:** 659-663.

Menounos, B.P. 2002. Climate, fine-sediment transport linkages, Coast Mountains, British Columbia. Ph.D. Thesis, Department of Geography, University of British Columbia, Vancouver B.C.

Muller, J. E. 1977. Geology of Vancouver Island. Geological Survey of Canada, Open File 463.

Muller, J.E., Northcote, K.E., Carlisle, D., 1974. Geology and mineral deposits of Alert Bay-Cape Scott map-area, Vancouver Island, British Columbia. Geological Survey of Canada.

Muller, J. E., Northcote, K. E. and Carlisle, D. 1974. Geology and mineral deposits of Alert Bay-Cape Scott map area, Vancouver Island, British Columbia. 74-8.

Mulvaney, J. and Kamminga, J. 1999. The Prehistory of Australia. Smithsonian Institution Press.

Nagorsen, D. W. 2004. The rodents and lagomorphs of British Columbia. *In* Royal British Columbia Handbook. University of British Columbia Press.

Nagorsen, D. W. and Keddie, G. 2000. Late Pleistocene mountain goats (Oreamnos americanus) from Vancouver Island: biogeographic implications. Journal of Mammalogy. **81:** 666-675.

Nagorsen, D. W., Keddie, G. and Luszcz, T. 1996. Vancouver Island Marmot Bones in Subalpine Caves: Archaeological and Biological Implications. Occupational Paper no. 4, Ministry of Environment, Land and Parks/BC Parks, Victoria B.C..

Nesje, A., Dahl, S. O., Andersson, C. and Matthews, J. A. 2000. The lacustrine sedimentary sequence in Sygneskardvatnet, western Norway; a continuous, high-resolution record of the Jostedalsbreen ice cap during the Holocene. Quaternary Science Reviews. **19:** 1047-1065.

Porter, S.C. and Swanson, T.W., 1998. Radiocarbon age constraints on rates of advance and retreat of the Puget Lobe of the Cordilleran Ice Sheet during the last glaciation. Quaternary Reasearch. **50:** 205 213

Prest, V. K. 1969. Retreat of Wisconsin and recent ice in North America. Geological Survey of Canada, Map 1257 A,.

Ramsey, C. L., Griffiths, P. A., Fedje, D. W., Wigen, R. J. and Mackie, Q. 2004. Preliminary investigations of a late Wisconsinan fauna from K1 cave, Queen Charlotte Islands (Haida Gwaii), Canada. Quaternary Research. **62:** 105-109.

Smith, J. G. 2003. Aspects of the loss-on-ignition (LOI) technique in the context of clay-rich, glaciolacustrine sediments. Geografiska Annaler. **85:** 91-97.

Stuiver, M. and Reimer, P. J. 1993. Extended ^{14}C database and revised CALIB radiocarbon calibration program. Radiocarbon. **35:** 215-230.

Stuiver, M., Reimer, P. J., Bard, E., Beck, J. W., Burr, G. S., Hughen, K. A., Kromer, B., MacCormac, F. G., Plicht, J. and Spurk, M. 1998. INTCAL98 radiocarbon age calibration 24, 000-0 cal BP. Radiocarbon. **40:** 1041-1083.

Valen, V., Larsen, E. and Mangerud, J. 1995. High resolution paleomagnetic correlation of Middle Weichselian ice-dammed lake sediments in two coastal caves, western Norway. Boreas. **24:** 141-153.

Valen, V., Mangerud, J., Larsen, E. and Hufthammer, A. K. 1996. Sedimentology and stratigraphy in the cave Hamnsundhelleren, western Norway. Journal of Quaternary Science. **11:** 185-201.

Van Hoesen, J. G. and Orndorff, R. L. 2004. A comparative study on the micromorphology of glacial and nonglacial clasts with varying age and lithology. Canadian Journal of Earth Sciences. **41:** 1123-1139.

Verosub, K. L., Mehringer, P. J., Jr. and Waterstraat, P. 1986. Holocene secular variation in western North America; paleomagnetic record from Fish Lake, Harney County, Oregon. Journal of Geophysical Research. **91:** 3609-3623.

Ward, B. C. and Thomson, B. 2004. Late Pleistocene stratigraphy and chronology of lower Chehalis River valley, southwestern British Columbia; evidence for a restricted Coquitlam Stade. Canadian Journal of Earth Sciences. **41:** 881-895.

Ward, B. C., Wilson, M. C., Nagorsen, D. W., Nelson, D. E., Driver, J. C. and Wigen, R. J. 2003. Port Eliza cave: North American west coast interstadial environment and implications for human migrations. Quaternary Science Reviews. **22:** 1383-1388.

Youngman, P. M. and Schueler, F. W. 1991. *Martes nobilis* is a synonym of *Martes americana*, not an extinct Pleistocene-Holocene species. Journal of Mammalogy. **72:** 567-577.

APPENDICES

All appendices can be found on the accompanying CD-ROM.

Contents